N70 31787

NASA TECHNICAL MEMORANDUM

NASA TM X-52850

NASA TM X-52850

PRELIMINARY ANALYSIS TO DETERMINE THE REENTRY INSULATION REQUIREMENTS ON A PIONEER-TYPE HEAT SOURCE FOR USE IN THE ISOTOPE BRAYTON APPLICATION

by Raymond K. Burns
Lewis Research Center
Cleveland, Ohio
June 1970

CASE FILE COPY

This information is being published in preliminary form in order to expedite its early release

PRELIMINARY ANALYSIS TO DETERMINE THE REENTRY INSULATION REQUIREMENTS ON A PIONEER-TYPE HEAT SOURCE FOR USE IN THE ISOTOPE BRAYTON APPLICATION

by Raymond K. Burns

Lewis Research Center
Cleveland, Ohio

NATIONAL AERONAUTICS AND SPACE ADMINISTRATION

ABSTRACT

A systematic analytical approach to determine the thermal property requirements of the reentry protection on isotope heat sources is presented. Such an approach is necessary in order to satisfy both reentry and steady state thermal requirements in present heat source designs in which heat is transferred through the reentry materials during power system operation. Results are presented for a Pioneer-type heat source which is being considered for the Isotope Brayton application. These results indicate that the range of thermal properties of the heat source reentry materials which will result in acceptable temperatures during reentry and during steady state Brayton power system operation is very limited.

E-5784

PRELIMINARY ANALYSIS TO DETERMINE THE REENTRY INSULATION REQUIREMENTS ON A PIONEER-TYPE HEAT SOURCE FOR USE IN THE ISOTOPE BRAYTON APPLICATION

By Raymond K. Burns

Lewis Research Center

E-5784

SUMMARY

A systematic analytical approach to determine the thermal property requirements of the reentry protection on isotope heat sources is presented. Such an approach is necessary in order to satisfy both reentry and steady state thermal requirements in present heat source designs in which heat is transferred through the reentry materials during power system operation. Results are presented for a Pioneer-type heat source which is being considered for the Isotope Brayton application. These results indicate that the range of thermal properties of the heat source reentry materials which will result in acceptable temperatures during reentry and during steady state Brayton power system operation is very limited.

INTRODUCTION

A Brayton cycle power system is currently being developed by NASA Lewis Research Center for generation of auxiliary electrical power in space (see ref. 1). One of the energy sources being considered for this system is radioisotopes. In this case, the heat source unit (HSU) consists of a circular, planar array of heat sources (HS), figure 1, each of which contains isotope fuel (see ref. 2).

The HSU radiates thermal energy to the heat source heat exchanger (HSHX). The Brayton cycle working fluid is heated to the turbine inlet temperature, 1600° F, as it flows through the HSHX. The entire HSU is an integral part of a reentry vehicle (HSRV). Should atmospheric reentry ever occur, the HSRV is designed to insure safe, intact reentry of the HSU. In addition, should an individual HS ever become separated from the HSU and HSRV it is provided with the capability of safe reentry by its own individual reentry protection material. Within the reentry materials, each HS contains a refractory metal capsule into which the isotope fuel is loaded.

Since the heat generated in the fuel must be transferred through the HS reentry protection, the presence of this material increases the capsule temperatures during power system operation. Since increased reentry protection results in increased steady state operating temperatures, these materials must be chosen to simultaneously satisfy both reentry and steady state thermal requirements. In the present analysis, a parametric approach is presented to determine the thermal properties of the HS reentry material which satisfy both requirements. Some examples are given for the Brayton application. They are not comprehensive but are intended only to illustrate the approach and to indicate the severity of the problem in meeting both requirements in the Brayton application using the present type of HS reentry protection design.

BRAYTON HEAT SOURCE THERMAL CONSTRAINTS

The AEC is developing an isotope thermoelectric generator for the Pioneer mission. A Pioneer-type HS is being considered for use in the Brayton HSU. As shown in figure 2, the capsule is surrounded by a hexagonal prism shaped POCO graphite reentry protection material. Between the capsule and the POCO, a sleeve of insulating material is included and completely surrounds the cylindrical portion of the capsule. The insulating material is necessary as a result of the requirement that the platinum-20% rhodium oxidation resistance clad on the tantalum alloy (T-111) strength member of the capsule not be allowed to reach its melting temperature ($\sim$3400^{o} F) during reentry.

For the Pioneer application, the reentry insulation currently being evaluated consists of three layers of pyrolytic graphite (PG) with a total thickness of 200 mils. In that case, the HS is required to survive, without platinum clad melting, a super-orbital reentry in a side-on-stable, flat side leading orientation. This orientation mode is generally accepted to be the most severe thermally. In the Pioneer application the HS contains 875 watts thermal of fuel. Heat is transferred axisymmetrically from the HS to a sink temperature of approximately 1100^{o} F.

In the Brayton application each HS contains 400 watts thermal of fuel and heat is transferred from only one side of the HS planar array and the sink temperature (HSHX surface) is above 1600^{o} F. Operation temperatures in the Brayton application will be higher than in the Pioneer application. For Brayton, the temperature limitation on the T-111 structural member of the capsule has been assumed for this study to be 2200^{o} F. Steady state thermal calculations have shown that the T-111 temperature reaches about 2000^{o} F

even when no insulating material is included, i.e., when the reentry protection consists of only POCO with emissivity of 0.8 and thermal conductivity of ~20.0 BTU/hr-ft-^{o}F at 2000^{o} F. When the Pioneer insulation, three layers of PG (with thermal conductivity < 1.0 BTU/hr-ft-^{o}F), is included the assumed temperature limit is appreciably exceeded. The T-111 operating temperature, when PG insulation is included, can be kept below 2200^{o} F by either reducing fuel loading or increasing capsule length. The other obvious alternative would be to reduce the amount of insulation, which would then result in decreased reentry capacity.

THERMAL ANALYSIS

Parametric Analysis of the Reentry Insulation

For individual HS reentry, protection materials with low thermal diffusivity, i.e., low conductivity and high heat capacity, are required. Yet during power system operation, the same protection material is required to have as high a thermal conductivity as possible. Clearly a tradeoff between these two requirements is necessary. The thermal properties required of the reentry protection in order to meet both requirements can be determined in a systematic manner on one graph. This graph would show the peak clad temperature during reentry and the peak T-111 temperature during power system operation as a function of the effective thermal conductivity of the reentry material. On such a plot, the minimum thermal conductivity which would result in acceptable T-111 temperatures during operation (k_{SS}) and the maximum thermal conductivity which would result in acceptable clad temperatures during reentry (k_{RE}) could be read directly. If k_{RE} is greater than k_{SS}, the range between them would be the range of design values for which both temperature limitations are satisfied.

Such a plot would of course be a function of many other parameters such as initial reentry conditions and dynamic motion of the HS, 'ablative' properties of the reentry material, temperatures in the HS at initial reentry, HS fuel loading, HS orientation and spacing in the HSU, and the effective sink temperature to which the HSU radiates. In using this plot as a preliminary design tool, variation in each of these additional factors would result in a different graph. In the Brayton HSU application, however, many of these additional factors have already been fixed or limited. The exterior geometry of the HS, except the length, is currently specified; the fuel load is fixed at 400 watts, and the reentry protection materials were assumed to be POCO with a 200 mil insulating sleeve over the capsule. The HSHX temperature, the sink

temperature to which the HSU radiates, is fixed by the Brayton cycle turbine inlet temperature and the HSU is confined by size limitations to be a close-packed array.

Several examples of this peak temperature versus reentry protection conductivity plot are presented herein for the Brayton HSU application. Only orbital reentry velocities ($\sim$26,000 ft/sec) are considered. Side-on-stable, flat side leading and side-on-spinning orientations during reentry of the HS are examined. The reentry protection materials are taken as POCO with a 200 mil thick insulation sleeve over the cylindrical portion of the capsule. The thermal conductivity of the insulating sleeve is taken as the independent parameter. The effects of POCO surface recession on the HS temperatures or on the net input heat flux are not included.

For simplicity, to eliminate the necessity of determining the heating distribution around a hexagonal prism in cross flow, the outer envelope of the HS is assumed to be cylindrical with a diameter equal to the across flats dimension of the Pioneer HS.

Thermal Model

The two dimensional thermal model, a network of nodes representing one half of a HS, used in both the steady state operation and the reentry analysis is shown in figure 3. As previously explained, the hexagonal shape was taken as cylindrical. For the steady state analysis, the POCO graphite surfaces at the top half of the HS radiate to the HSHX which was taken to be at 1670^{o} F, the hot spot temperature predicted in reference 2. The radiative exchange factors between the HS and HSHX were calculated using an emissivity of 0.8 for POCO graphite and 0.85 for the HSHX. The presence of the adjacent HS was included in this calculation. The external surfaces of the POCO on the bottom half of a HS were assumed to be adiabatic, a slightly conservative approach.

For the reentry analysis, the external surfaces of the POCO graphite were subjected to a convective heat pulse using the heating ratios shown in figure 4. These are the ratios of local heating on a side-on-stable cylinder to that at the stagnation point of a one-foot radius sphere. In this analysis only, convective heating in continuum flow is considered and surface recession is neglected. The heating factors are therefore assumed to be constant throughout the heating pulse. In the case of the side-on-spinning mode the heating factors are all taken as the average of those given in figure 4. It is also assumed that all external POCO surfaces radiate to a 0^{o} F sink with an emissivity of 0.8.

The nodes in the region denoted in figure 3 as reentry insulation were assumed to have a temperature dependent heat capacity identical to POCO. The thermal conductivity of these nodes was varied parametrically. It was assumed that there is a radiation gap between the POCO and the insulation and between the insulation and the clad. The emissivity of the POCO was taken as 0.8 and of the clad as 0.85. Two values, 0.5 and 0.8, were taken as the emissivity of the insulation material. During reentry, the presence of a gas such as air or CO in these gaps, or the presence of partial contact between the surfaces, would increase the capsule temperatures. This was not considered in the present analysis.

Since clad melting during reentry was considered a failure, emphasis was not placed on temperatures occurring after such an event. Therefore, the effects of the heat of fusion of the platinum-20% rhodium clad was not included. As a result, when the melt temperature is reached, the expected plateau in clad temperature is not predicted.

The temperature distributions for both reentry and steady state operating conditions were determined using this thermal model and the CINDA-3G (ref. 4) computer code.

It is recognized that in order to simulate the actual capsule during steady state operation using the present two-dimensional model, an effective power density of the fuel in the model must be used. This effective power density is obtained by dividing the HS fuel loading by the effective volume of the fuel. The effective volume is a function not only of the capsule dimensions but of the three-dimensional heat transfer at the HS ends. Two possible approaches are: (1) to take the effective volume as the volume of the cylindrical portion of the fuel cavity, and (2) to take the effective volume as the sum of the cylindrical volume and the volume of the hemispherical void in the capsule ends. The first approach would be conservative because it takes no account for longitudinal heat transfer. The second approach is optimistic since the end region voids will not actually be completely filled and the capsule ends are surrounded by low thermal conductivity tantalum felt compliance pads.

In figure 5 the effective power density for these two cases is plotted as a function of overall capsule length for a 400 watt loading. The broken line was estimated by comparing two-dimensional calculations similar to the present ones with three-dimensional results given in reference 3 for the Pioneer application. The effective power density given by the broken line is used in this analysis.

RESULTS AND DISCUSSION

Steady State Operating Conditions

In figures 6 through 11 steady state operating temperatures are given for reentry insulation conductivities of 1.0, 5.0, and 20.0 BTU/hr-ft-^{o}F and reentry insulation emissivities of 0.5 and 0.8. In each case two sets of curves are given. One shows the key hot spot temperatures and the other gives the temperatures radially through the reentry materials at the top of the HS. The temperatures are given as a function of effective power density of the fuel and must be related to the actual capsule by use of figure 5. For example, the figures showing the hot spot temperatures together with figure 5 (or curves similar to figure 5 for different capsule loadings) can be used to determine the steady state capsule temperatures as a function of length (or loading). The data given in these figures will later be used to illustrate the parametric approach to determine the acceptable range of reentry insulation thermal properties.

The figures showing the radial temperature profiles at the top of the HS clearly show the thermal penalty of the thermal insulation and the radiation gaps in each case. For a thermal conductivity of the 200 mil insulating sleeve of 1.0 BTU/hr-ft-^{o}F (fig. 6b) the temperature gradient through the insulation material is of the order of magnitude of the temperature increase across one of the radiation gaps. For an insulation conductivity of 20.0 BTU/hr-ft-^{o}F (fig. 8b) a value approximating that of POCO, the gradient through the material is small. However, in any case, the thermal penalty of the radiation gap remains. The advantage in keeping the insulation emissivity high is shown by comparison of the cases in figures 8b and 11b, for which the temperature gradients through the insulation are small and the major thermal penalty is the radiation gaps. For the lower emissivity value, in figure 11b, the temperature increase caused by the radiation gaps is significantly higher than that caused by the gaps in the higher emissivity case of figure 8b.

Reentry of an Individual HS

For the reentry results presented here, initial reentry angles of -0.5^{o} (representative of long, shallow trajectories) and -2.15^{o} (representative of shorter trajectories which result in higher POCO surface temperatures) were chosen. The convective pulses to the stagnation point of a one-foot radius sphere are given in figures 12 and 13 for these two initial reentry angles. The heating factors in figure 4 were used to relate the pulse on the thermal model to the pulses given in figures 12 and 13.

In figures 14 through 22 the temperature gradients through the reentry materials and the T-111 and Pt-20% Rh clad temperatures on the leading side during reentry are given for insulation conductivities of 1.0, 5.0, and 20.0 BTU/hr-ft-^{o}F and emissivities of 0.5 and 0.8. The temperatures in figures 14 through 19 correspond to reentry from orbit at initial angle of -2.15^{o} and those in figure 20 through 22 correspond to the smaller angle considered, -0.5^{o}. For the smaller reentry angle cases, only the higher insulation emissivity case (the case which results in higher peak capsule temperatures) was considered. The HS length and effective power density of the fuel are not noted in figures 14 through 22 for the following reasons: (1) a two-dimensional model was used, (2) the effect of fuel power density is small compared to aerodynamic heating, and (3) the ballistic coefficient was arbitrarily fixed making the convective pulse independent of the HS length. Also, as previously explained, the analysis does not include the effect of clad heat of fusion and the predicted clad temperatures in figures 14 through 22 reflect this omission when the melt temperature is reached. The HS temperature distribution at initial reentry was the same in each case and roughly corresponds to the steady state radial distribution of an individual HS exposed to space.

Quantitative comparisons between the thermal results for the two trajectories considered should be made carefully since the amount of surface recession will be different in the two cases, and as already noted, this effect has not been included. The results, however, do illustrate, as expected, that the peak POCO surface temperature is much lower for the shallower trajectory and that since the shallower trajectory is much longer in time, it results in a smaller difference between peak POCO surface temperature and peak clad temperature.

The difference in the HS temperatures resulting from side-on-stable and side-on-spinning modes of reentry can be illustrated for one case by comparing figures 16 and 23. The clad does not reach melt temperature in the spinning case of figure 23 even though the insulation conductivity and emissivity are the highest considered here. The amount of insulation required to protect against side-on-stable reentry is considerably more than that required for spinning reentry.

Simultaneous Consideration of Steady State and Reentry Conditions

The results given in figures 6a through 11a and 14 through 22 can be combined to show peak clad and T-111 temperatures during reentry and steady state operation as a function of insulation conductivity and emissivity. These are given in figures 24 and 25 for reentry angles of -0.5^{o} and -2.15^{o} respectively. Steady state temperatures are included for two capsule lengths, 4.8 inch and 6.3 inch. The power densities given by the broken line in figure 5 were used and the results must therefore be considered preliminary pending a better assessment of three dimensional effects. The reentry temperatures are not given for different lengths since the effect on predicted reentry temperatures is small as previously explained.

The steady state temperatures in figures 24 and 25 show a decreasing rate of change with increasing insulation conductivity. Reference to figures 9b and 11b provides the explanation. As the conductivity of the insulation is increased, only the thermal penalty of the radiation gap remains and the T-111 temperature becomes relatively independent of the insulation conductivity. The temperatures during reentry are also indicated by figures 24 and 25 to become relatively independent of insulation conductivity at high conductivity values. Figures 14 through 22 show that the peak POCO surface temperature does not vary appreciably with changes in insulation conductivity and that at high values of insulation conductivity most of the thermal protection for the clad is provided by the radiation gaps which were assumed to exist between the reentry protection materials.

In figure 24 it is seen that for the 4.8 inch capsule length the T-111 temperature exceeds 2200^{o} F (the limit assumed for this study) for all insulation conductivities considered. For the 6.3 inch capsule the minimum conductivity which yields steady state T-111 operating temperatures less than 2200^{o} F is 1.2 BTU/hr-ft-^{o}F (denoted by the circle symbol). For this shallow reentry trajectory, all insulation conductivities considered, up to 20.0 BTU/hr-ft-^{o}F, resulted in acceptable clad temperatures. The acceptable range of insulation conductivities for this case would then be from 1.2 to over 20.0 BTU/hr-ft-^{o}F.

In figure 25 for an insulation emissivity of 0.8 the steady state temperatures are the same as in figure 24. It has already been noted that for the 6.3 inch capsule length the insulation conductivity must exceed 1.2 BTU/hr-ft-^{o}F to yield T-111 temperatures less than 2200^{o} F. For this case the maximum indicated conductivity which keeps the clad below its melting temperature

is 2.3 BTU/hr-ft-^{o}F (denoted by the square symbol). The acceptable range for this trajectory ($\gamma_E = 2.15^{o}$) would then be from 1.2 to 2.3 BTU/hr-ft-^{o}F.

For an insulation emissivity of 0.5 the situation in figure 25 is quite different. For a 6.3 inch length the insulation conductivity must be a minimum of 11.0 BTU/hr-ft-^{o}F (denoted by the diamond symbol) for a T-111 operating temperature under 2200^{o} F. The difference between this value and that for the higher insulation emissivity illustrates the sensitivity of the steady state thermal performance to radiation gaps and the emissivities of the bounding surfaces. The maximum allowable insulation conductivity for this reentry case is indicated by figure 25 to be about 3.8 BTU/hr-ft-^{o}F (denoted by the inverted triangle symbol). For this case there is no single acceptable thermal conductivity which will meet both reentry and steady state requirements. A 'thermal switch' material, i.e., a material with a steady state effective conductivity higher than its effective value at the higher temperatures during reentry (see ref. 5), is required. Another approach would be to reduce the need for simultaneous thermal consideration of both steady state and reentry conditions. This could be accomplished by shaping the POCO material such that the HS reenters in one predictable side-on-stable mode making reentry insulation necessary only on one side. Since the HSU radiates to the HSHX on only one side, the preferred reentry side, which would include the insulation material, could be oriented downward in the HSU array (away from the HSHX) without substantially affecting steady state performance. Such a concept, using the Pioneer capsule, is currently being evaluated.

CONCLUDING REMARKS

A systematic analytical approach to determine the thermal property requirements of the reentry protection on isotope heat sources was presented. Such an approach is necessary to satisfy both reentry and steady state thermal requirements in present HS designs in which heat is transferred through the reentry materials during power system operation. The effective thermal conductivity of the reentry materials is taken as an independent parameter. Steady state operation temperatures and temperatures during reentry are calculated as a function of this parameter to determine the range of values for which both steady state and reentry temperatures are acceptable.

Example calculations for a Pioneer type HS for Brayton application are presented. Reentry from orbit with entry angles of -0.5^{o} and -2.15^{o} are considered for side-on-stable HS reentry.

The side-on-spinning mode of HS motion is also included. The thermal conductivity of a 200 mil thick insulating sleeve over the capsule and within the POCO graphite is taken as the independent parameter. The effects of POCO surface recession are not included.

The results presented indicate:

(1) The radiation gap introduced into the HS by including a separate reentry insulation layer is a significant, and in some cases the most important, thermal penalty during steady state operation. The steady state temperatures are sensitive to the emissivities of the surfaces bounding these gaps. These emissivities must therefore be kept as high as possible and be well known in order to accurately predict performance.

(2) The radiation gaps assumed to exist in the HS reentry protection material during reentry provide a significant thermal protection of the capsule. Whether these will in fact remain pure radiation gaps during reentry should be investigated.

(3) The amount of reentry insulation required to protect the capsule during a side-on-stable dynamic mode is considerably greater than required for a side-on-spinning mode for the same trajectory.

(4) In using a Pioneer type HS for the Brayton application, the thermal requirements on the reentry insulation in order that the capsule is protected during side-on-stable reentry and that steady state operation temperatures are kept below 2200^{o} F, are very strict. Such a design will require very close thermal analysis, using well characterized materials, in order to have any safety margin. A design which would eliminate the need to simultaneously consider reentry and steady state temperatures in selection of reentry protection materials would be desirable.

APPENDIX

Nomenclature

HS	Heat source; metallic capsule containing isotope fuel surrounded by individual reentry protection material.
HSU	Heat source unit; planar array of heat sources and its supporting structure for use as Brayton engine energy source.
HSHX	Heat source heat exchanger.
HSRV	Heat source reentry vehicle; reentry protection for the heat source unit.
k	Thermal conductivity.
POCO	POCO graphite reentry material of a heat source.
PG	Pyrolytic graphite.
T-111	Tantalum alloy strength member of a capsule.
V_E	Initial reentry velocity.
α_E	Initial reentry angle.
ϵ	Emissivity.

Subscripts

RE INS	Refers to reentry insulation material.

REFERENCES

1. Brown, William J.: Brayton-B Power System - A Progress Report. Proceedings of the 4th Intersociety Energy Conversion Engineering Conference. AIChE, 1969, pp. 652-658.

2. Ryan, Richard L.; and Graham, John W.: Isotope Reentry Vehicle Design Study, Preliminary Design: Phase II. Rep. AVSD-0306-69-RR, Avco Corp. (NASA CR-72555), Aug. 1969.

3. Ramon, S.: Steady State Operating Temperatures of SNAP-19/Pioneer Heat Source. Memo. SN 19-SR-210, Teledyne Isotopes, Inc., 1970.

4. Lewis, D. R.; Gaski, J. D.; and Thompson, L. R.: Chrysler Improved Numerical Differencing Analyzer for 3rd Generation Computers. Rep. TN-AP-67-287, Chrysler Corp. (NASA CR-99595), Oct. 20, 1967.

5. Anon.: High Temperature Metal Thermal Switch Development Program First Quarterly Report, July-August 1969. Hittman Associates, Inc., Mar. 1970. (Work under contract AT(29-2)-2797.)

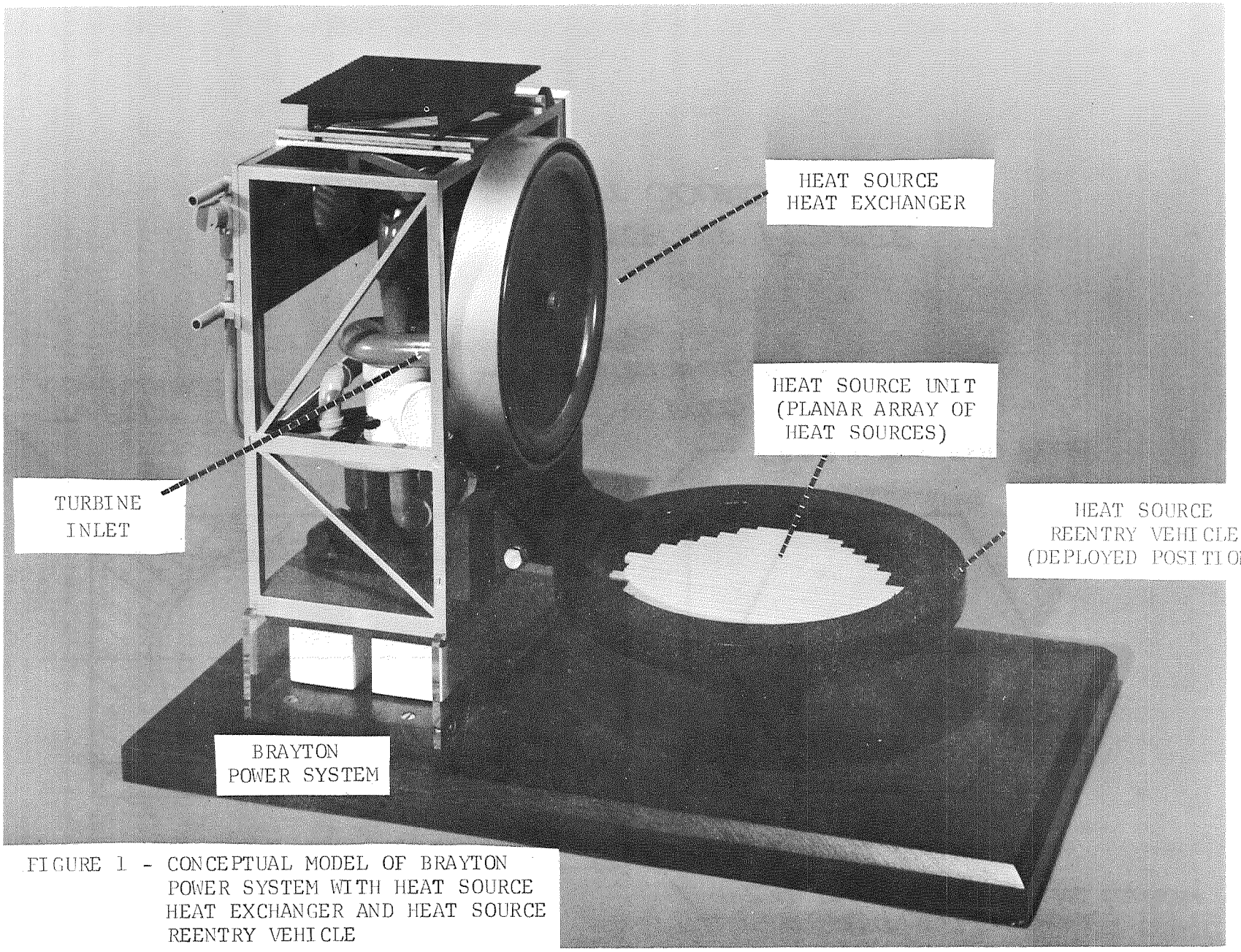

FIGURE 1 - CONCEPTUAL MODEL OF BRAYTON POWER SYSTEM WITH HEAT SOURCE HEAT EXCHANGER AND HEAT SOURCE REENTRY VEHICLE

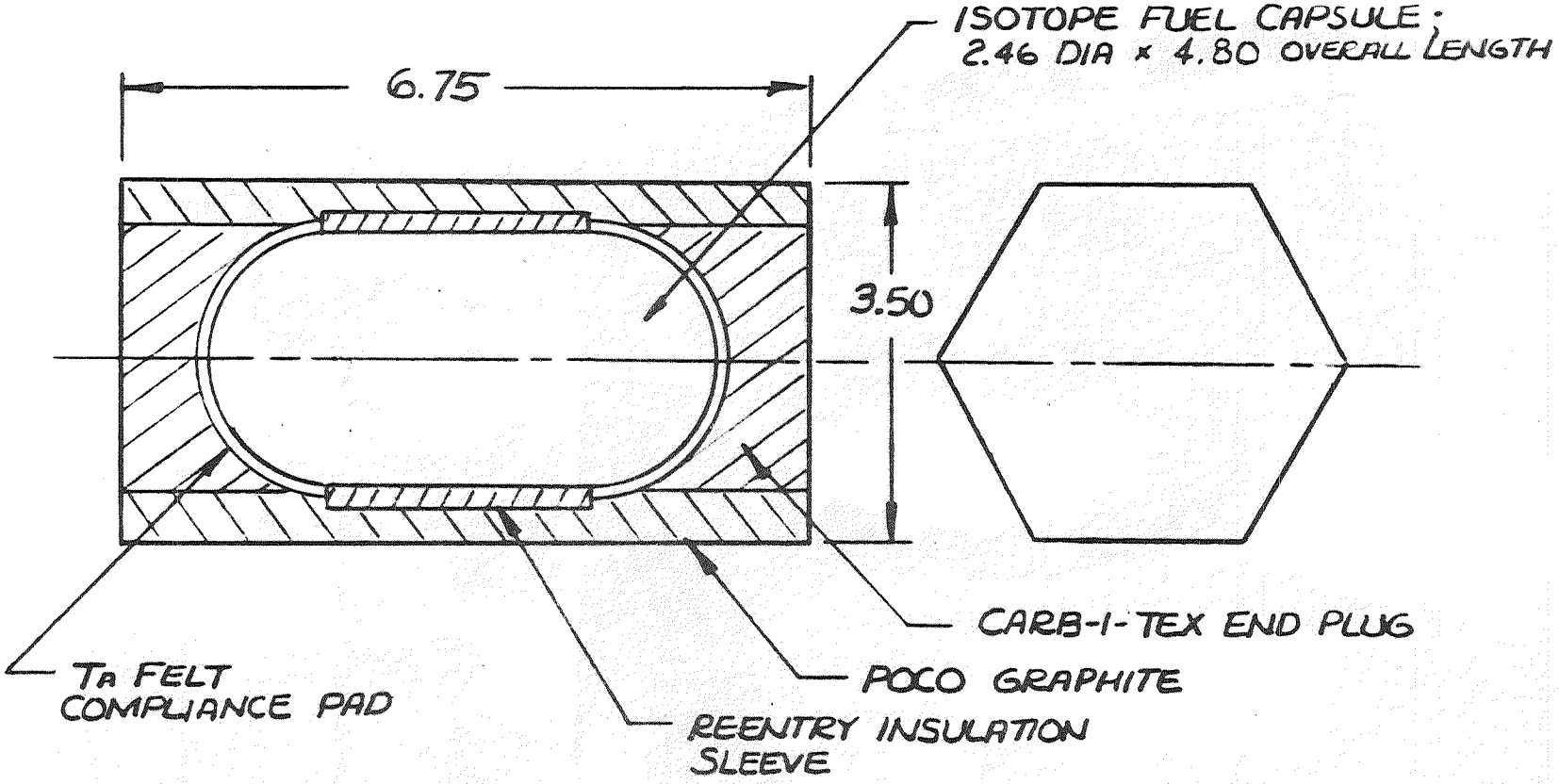

FIGURE 2 SKETCH OF PIONEER HEAT SOURCE

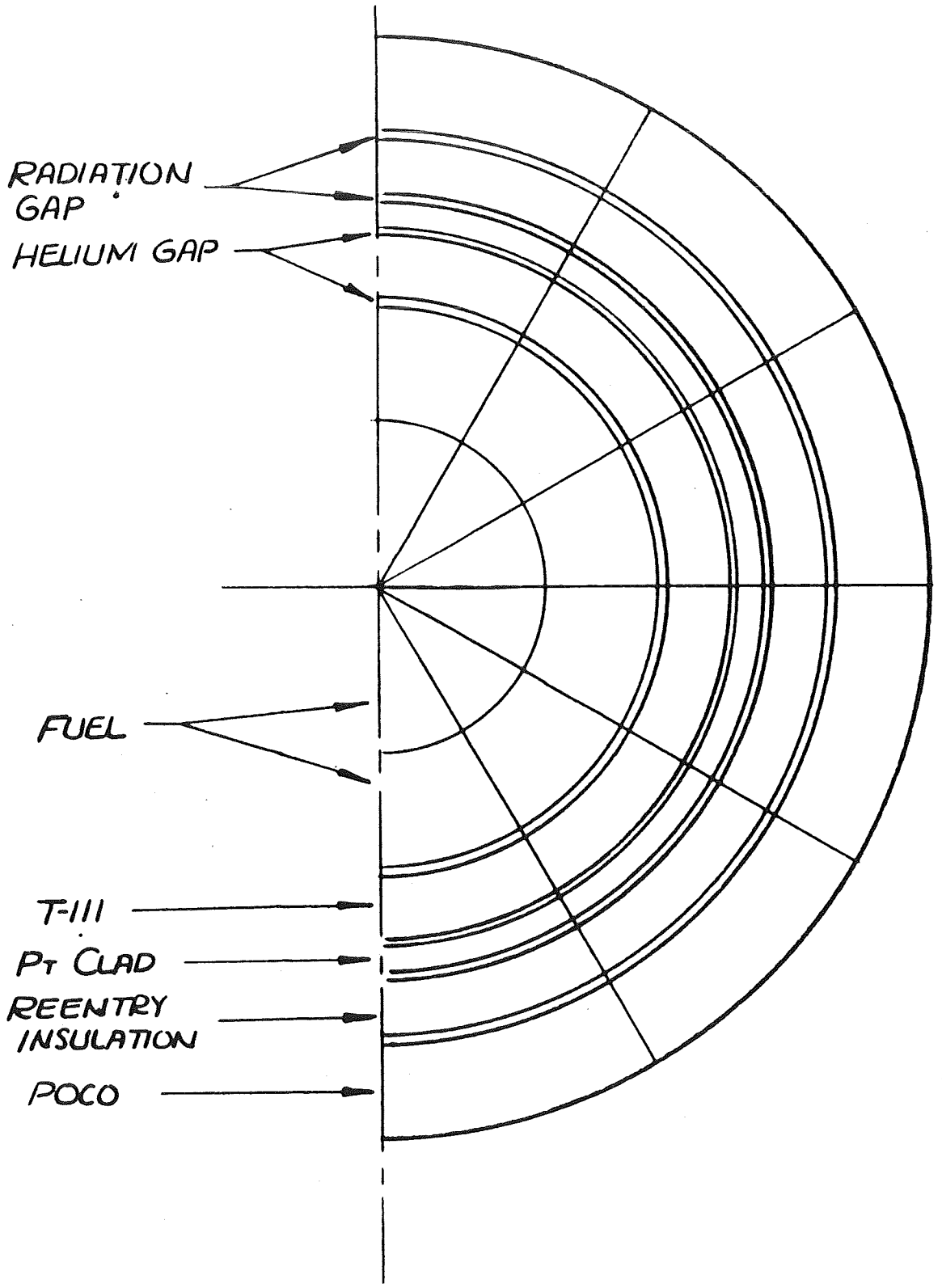

FIGURE 3 TWO DIMENSIONAL THERMAL MODEL

$$F \equiv \frac{\text{LOCAL HEAT FLUX}}{\text{HEAT FLUX TO STAGNATION POINT 1 FT SPHERE}}$$

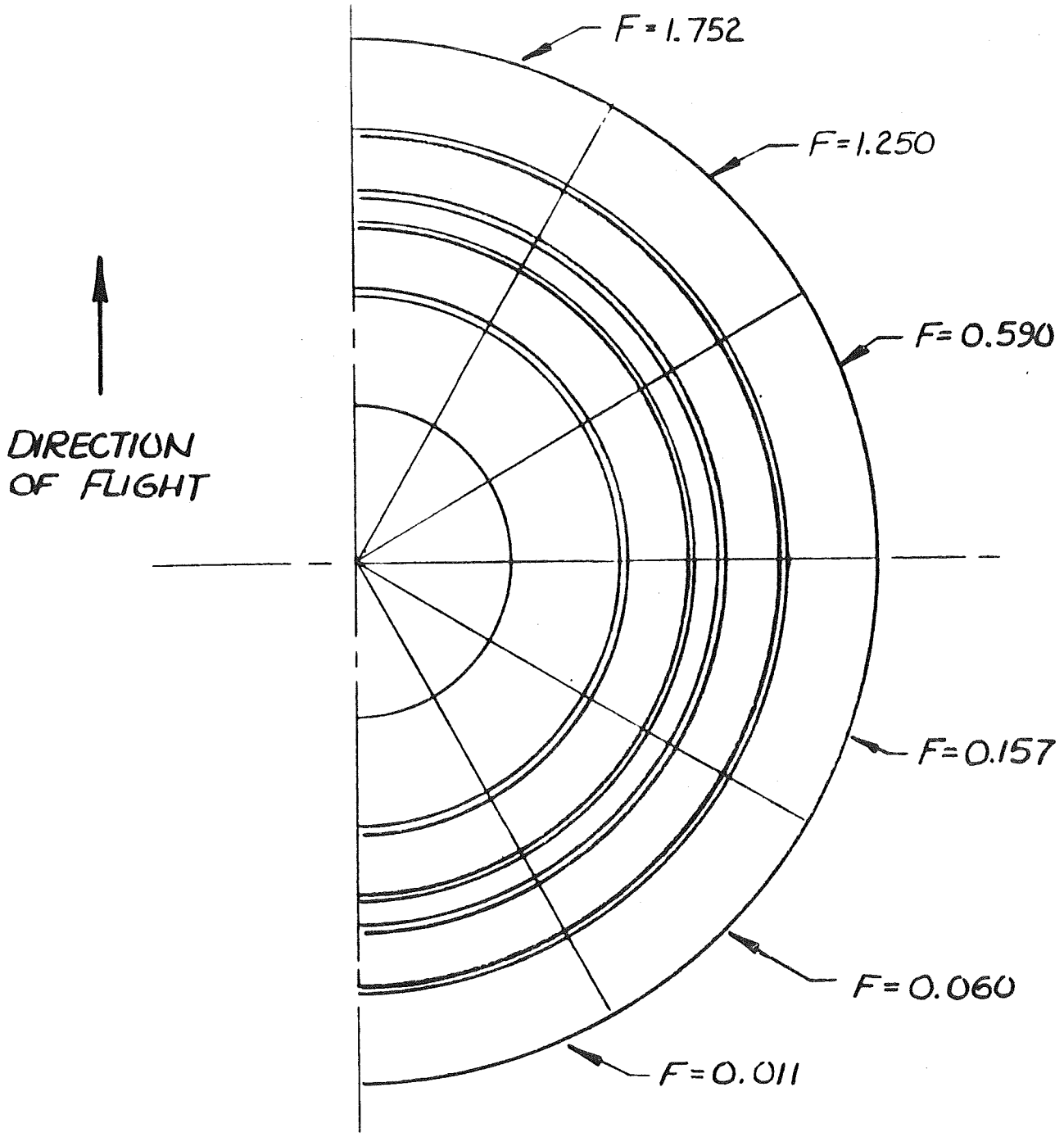

FIGURE 4 CONVECTIVE HEATING FACTORS; SIDE-ON - STABLE

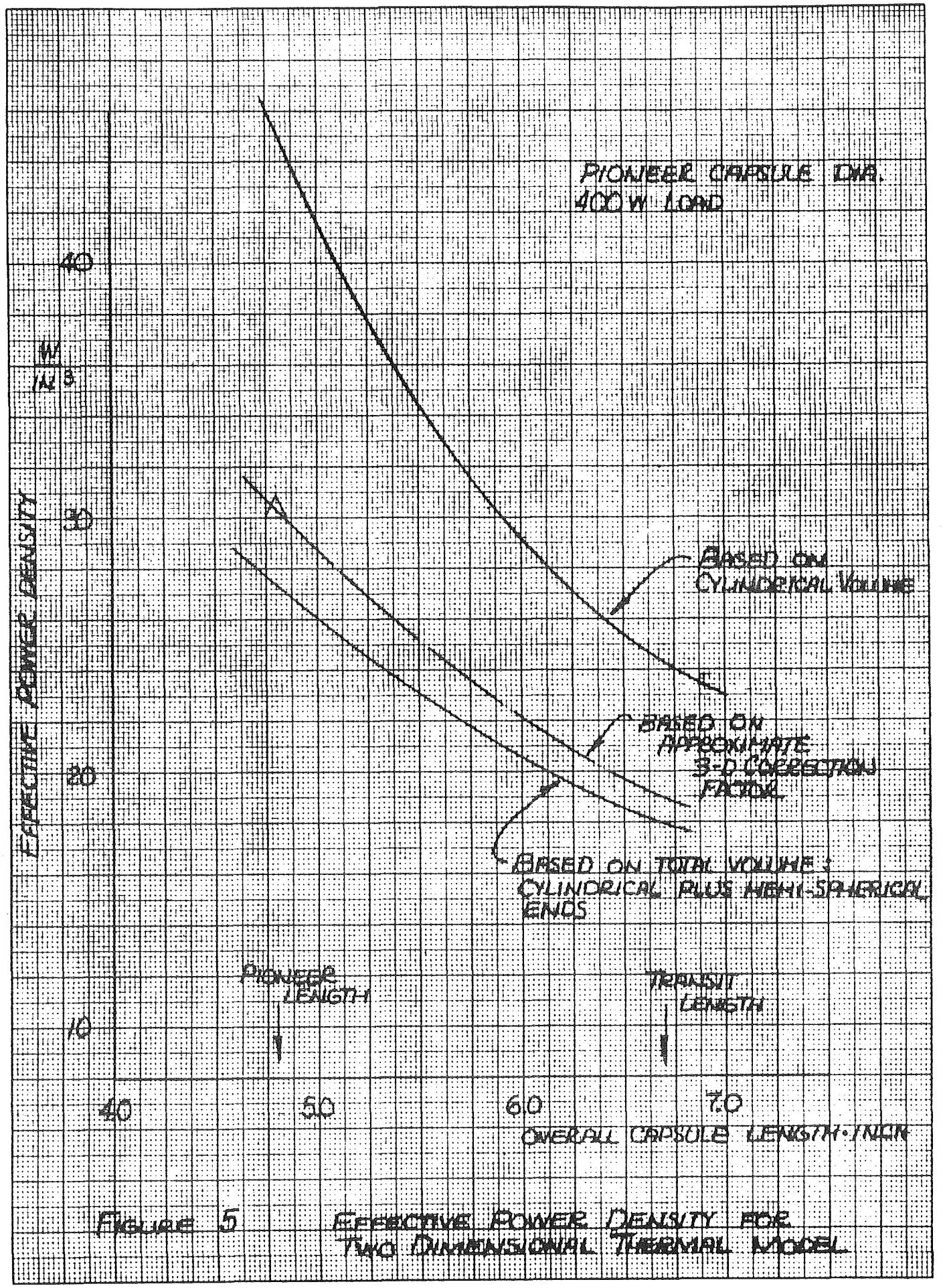

FIGURE 5 EFFECTIVE POWER DENSITY FOR TWO DIMENSIONAL THERMAL MODEL

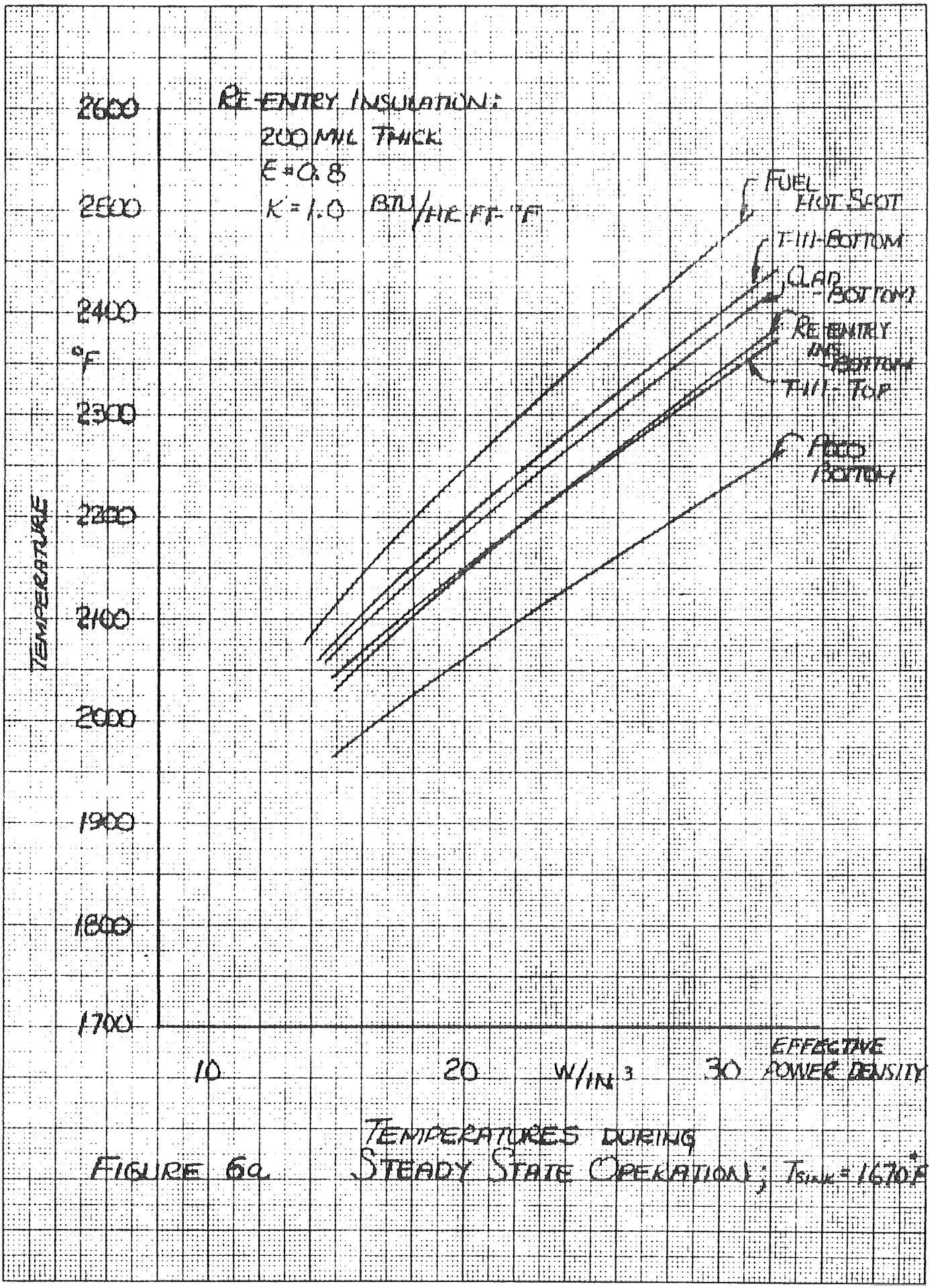

FIGURE 6a TEMPERATURES DURING STEADY STATE OPERATION; $T_{SINK} = 1670°F$

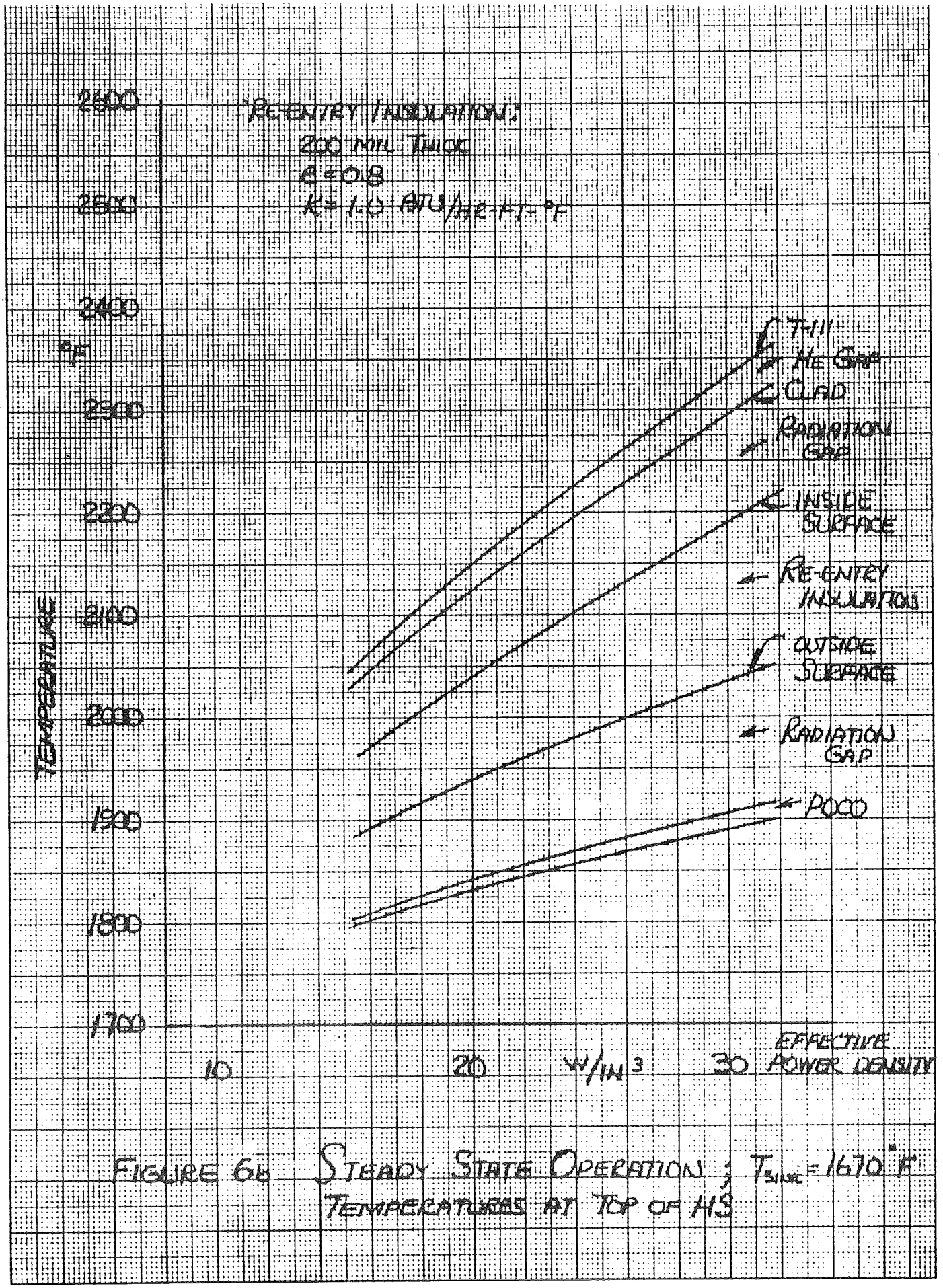

FIGURE 6b STEADY STATE OPERATION; T_{SINK} = 1670 °F
TEMPERATURES AT TOP OF HS

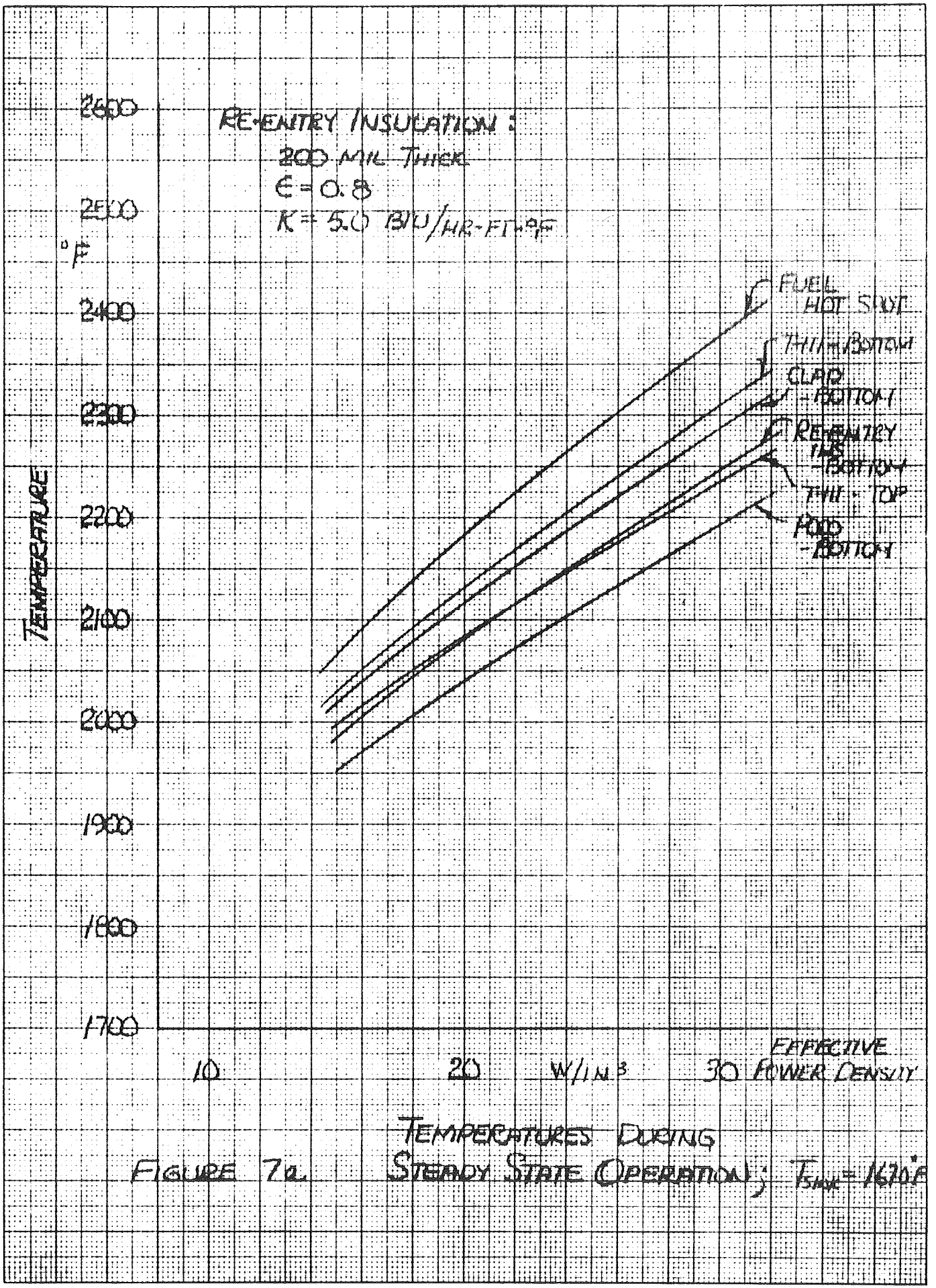

FIGURE 7a. TEMPERATURES DURING STEADY STATE OPERATION; T_{SINK} = 1610°F

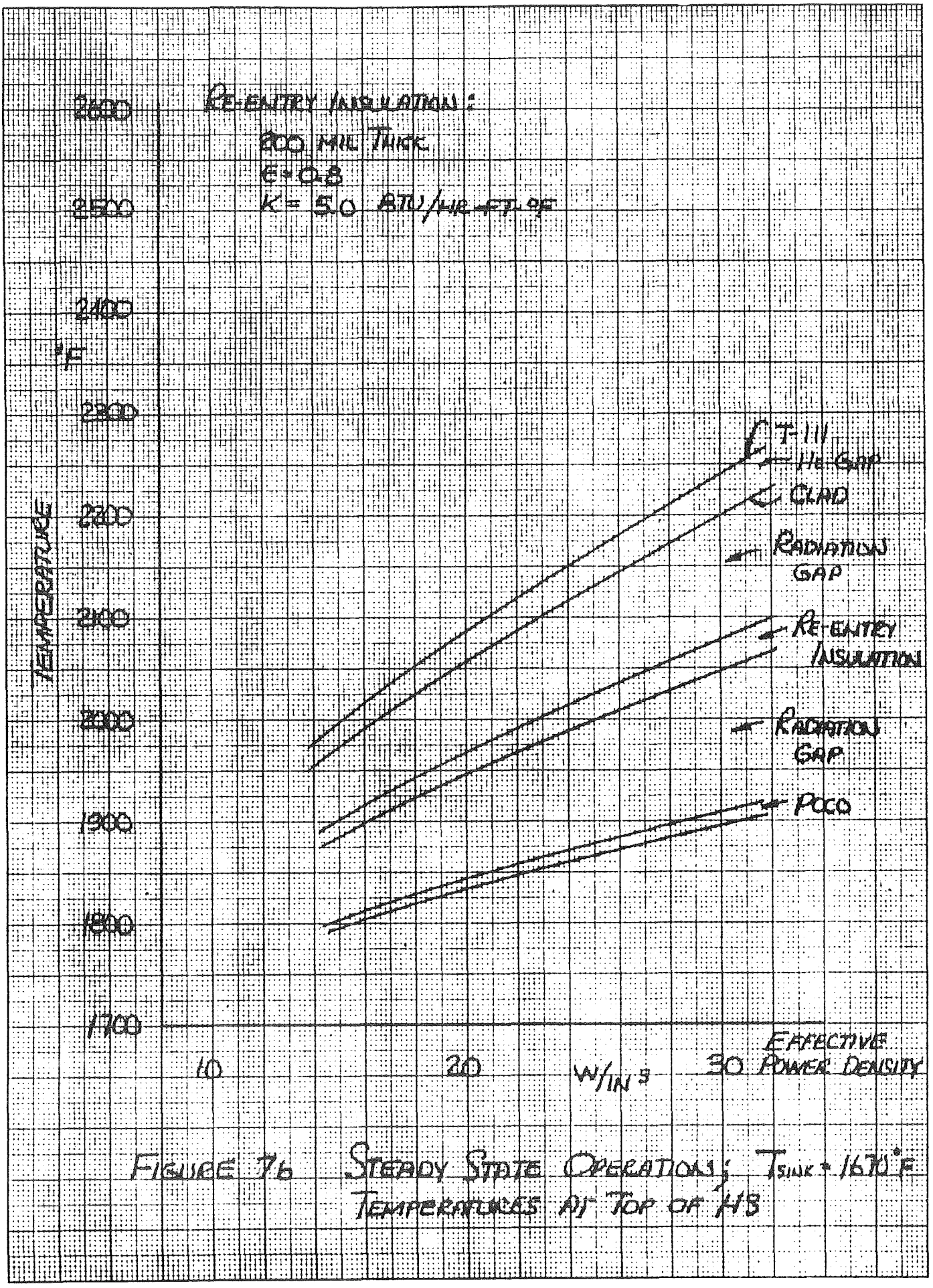

FIGURE 76 STEADY STATE OPERATION; T_{SINK} = 1670°F
TEMPERATURES AT TOP OF HS

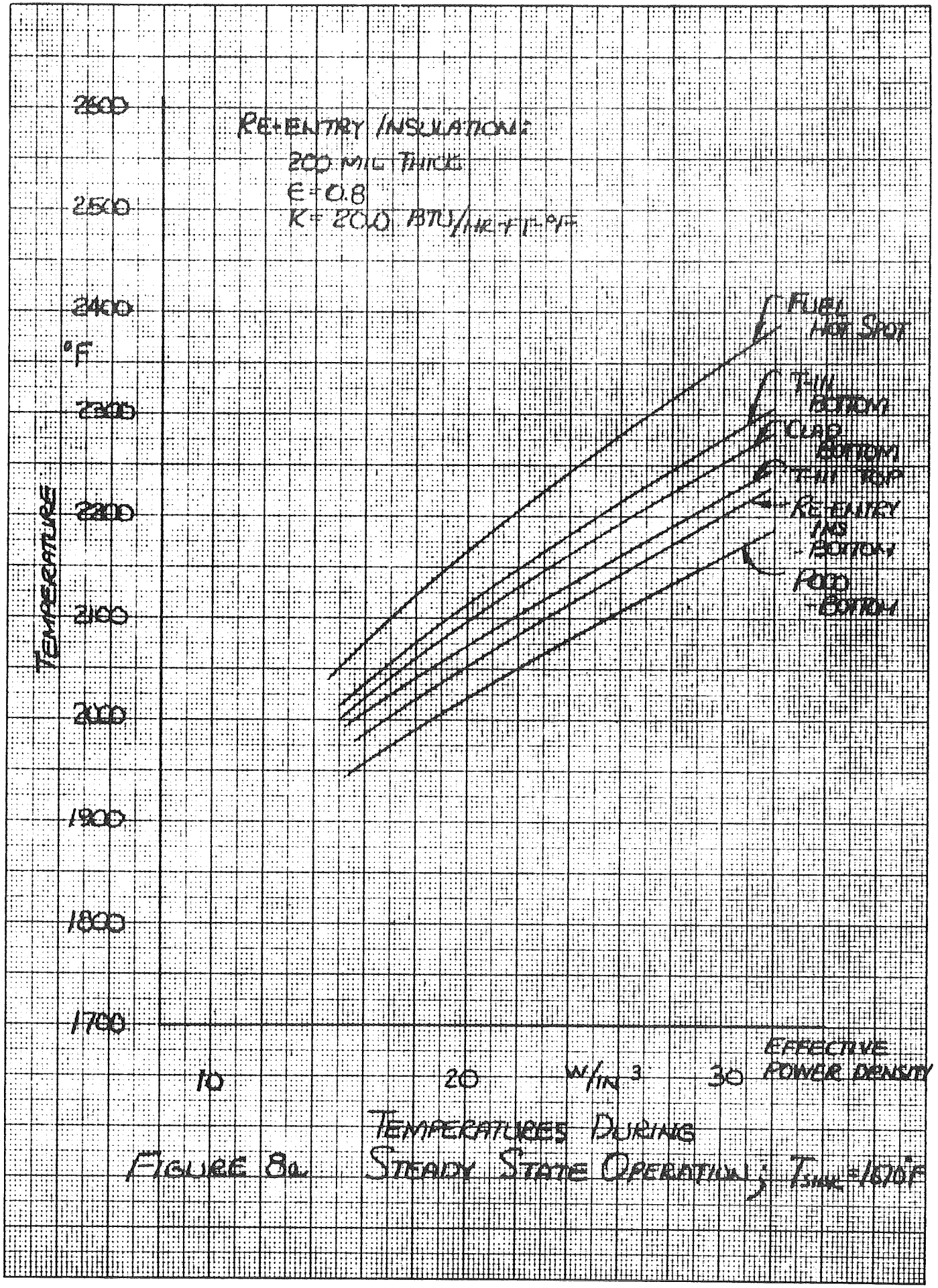

FIGURE 8a. TEMPERATURES DURING STEADY STATE OPERATION, $T_{SINK} = 160°F$

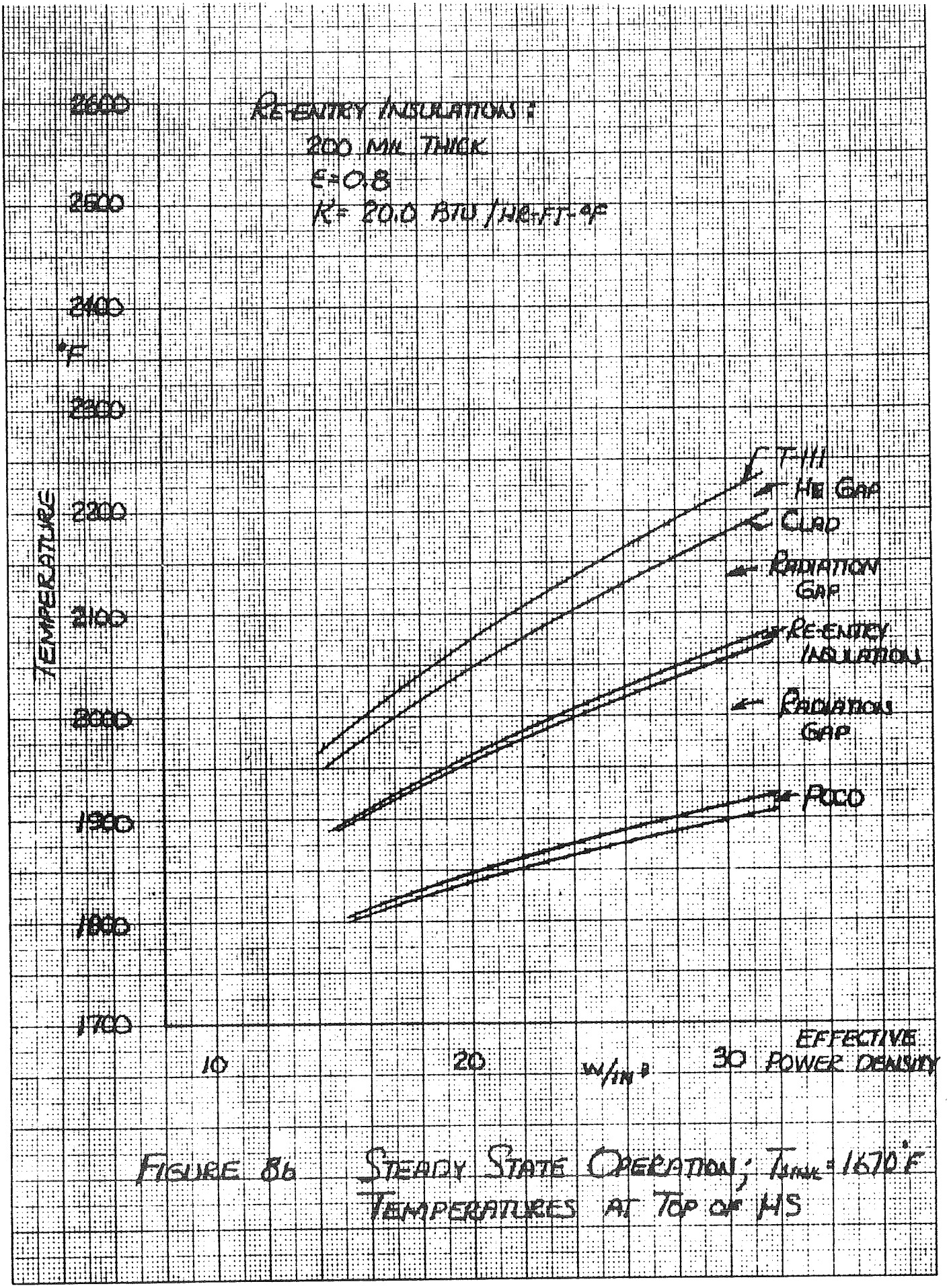

FIGURE 86 STEADY STATE OPERATION; T_{MAX} = 1670°F
TEMPERATURES AT TOP OF HS

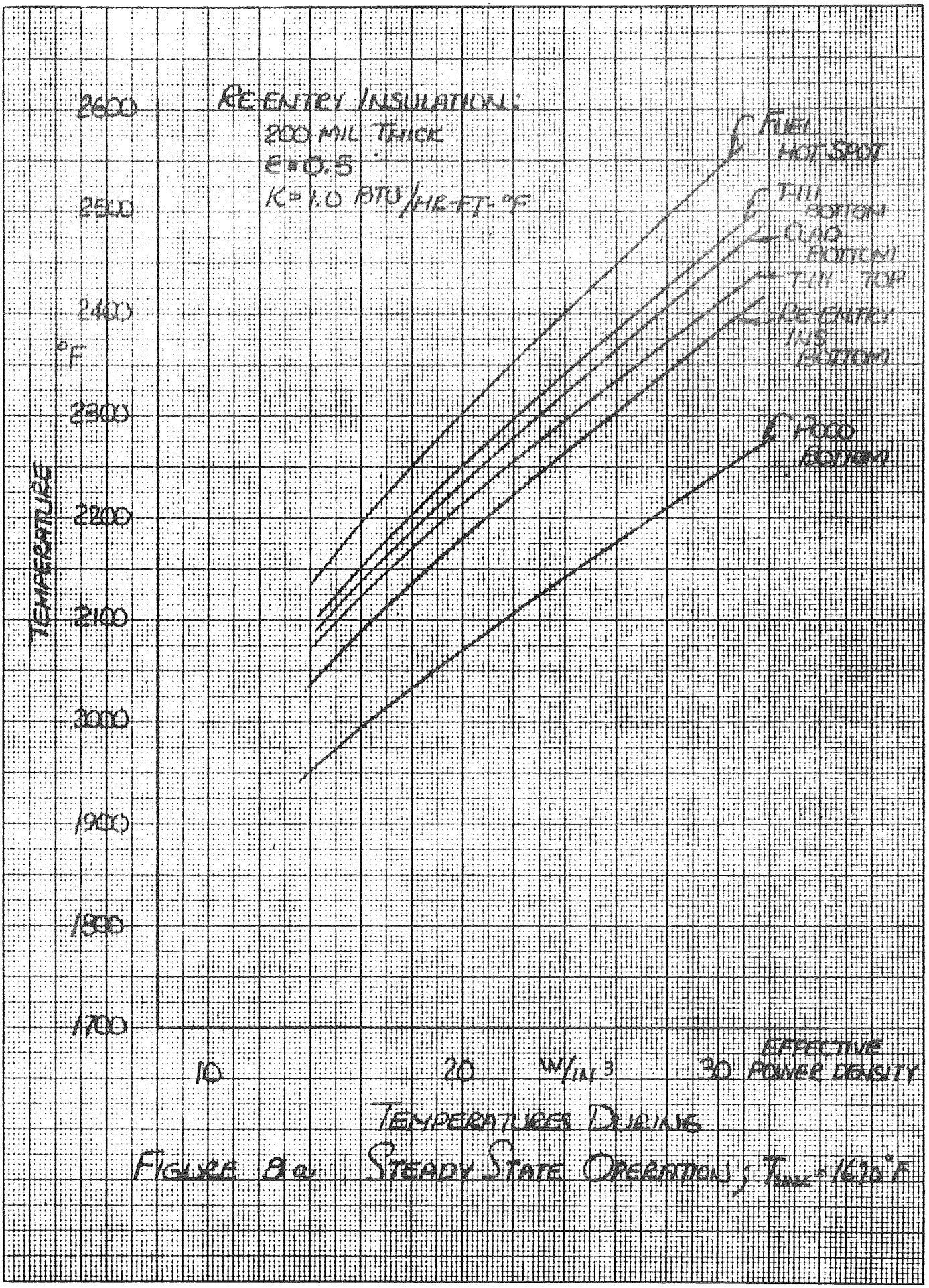

TEMPERATURES DURING

FIGURE 8a STEADY STATE OPERATION; $T_{MAX} = 1610°F$

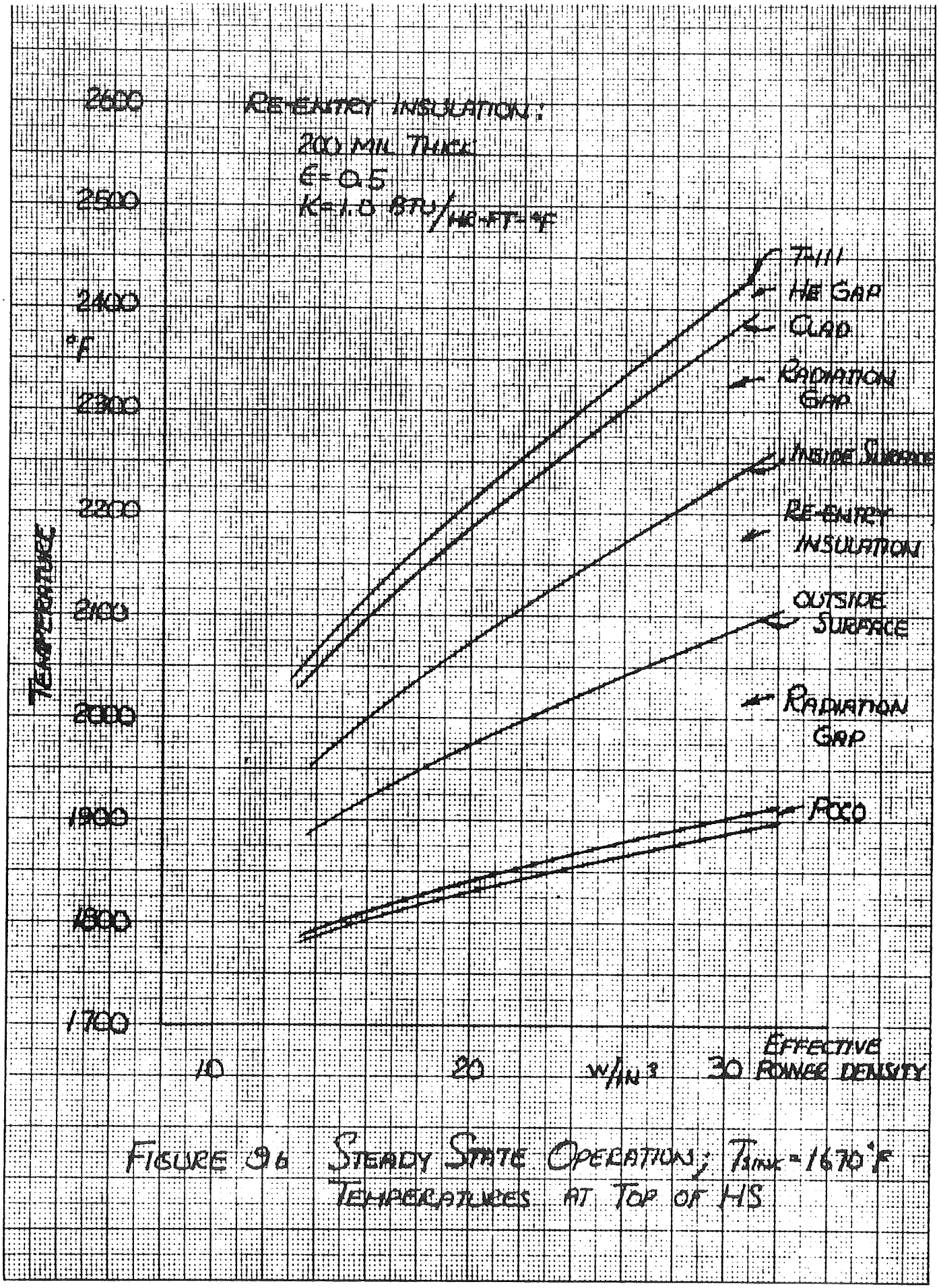

FIGURE 96 STEADY STATE OPERATION; $T_{SINK} = 1670°F$
TEMPERATURES AT TOP OF HS

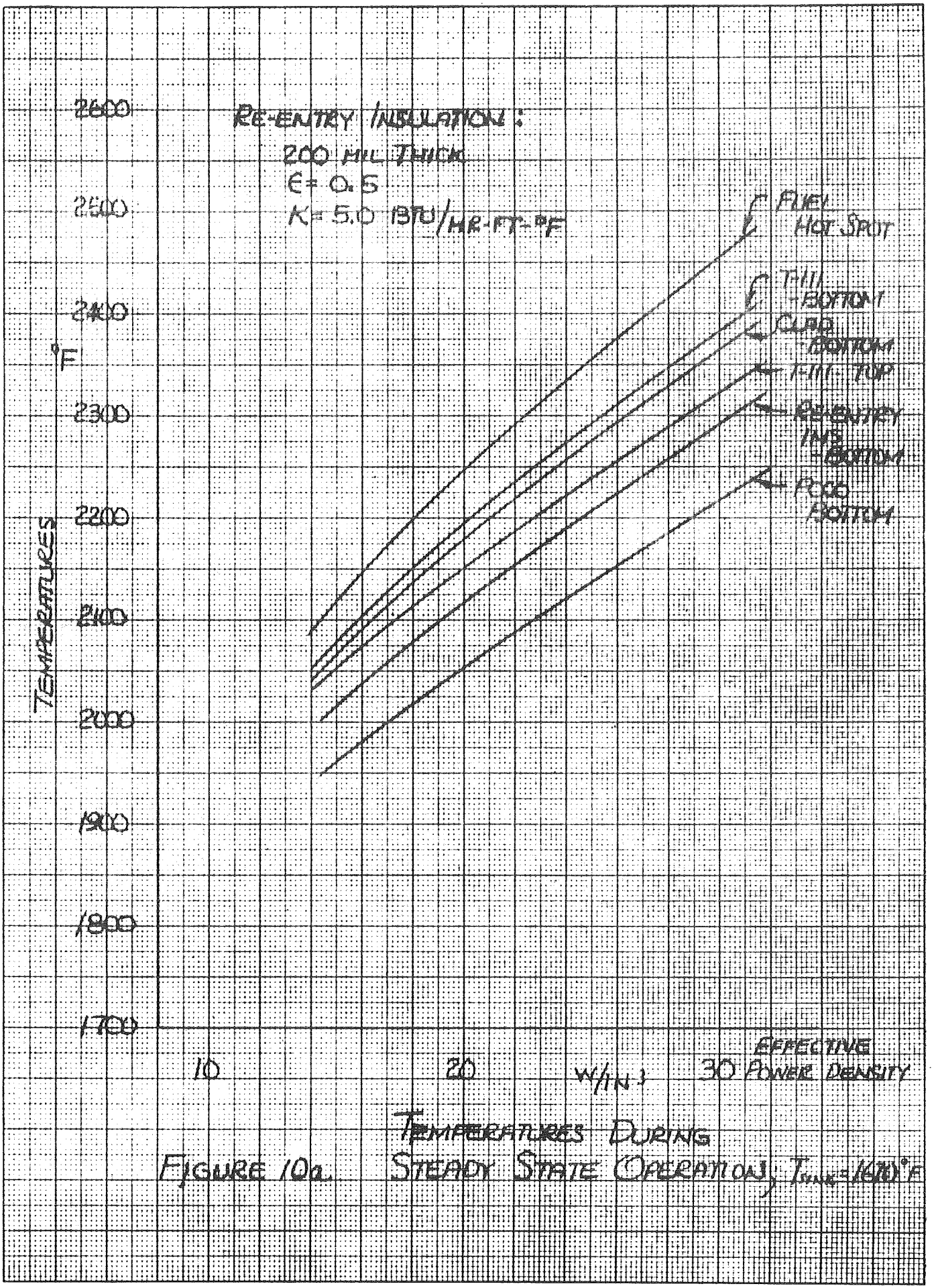

FIGURE 10a. TEMPERATURES DURING STEADY STATE OPERATION, $T_{LINE} = 1670°F$

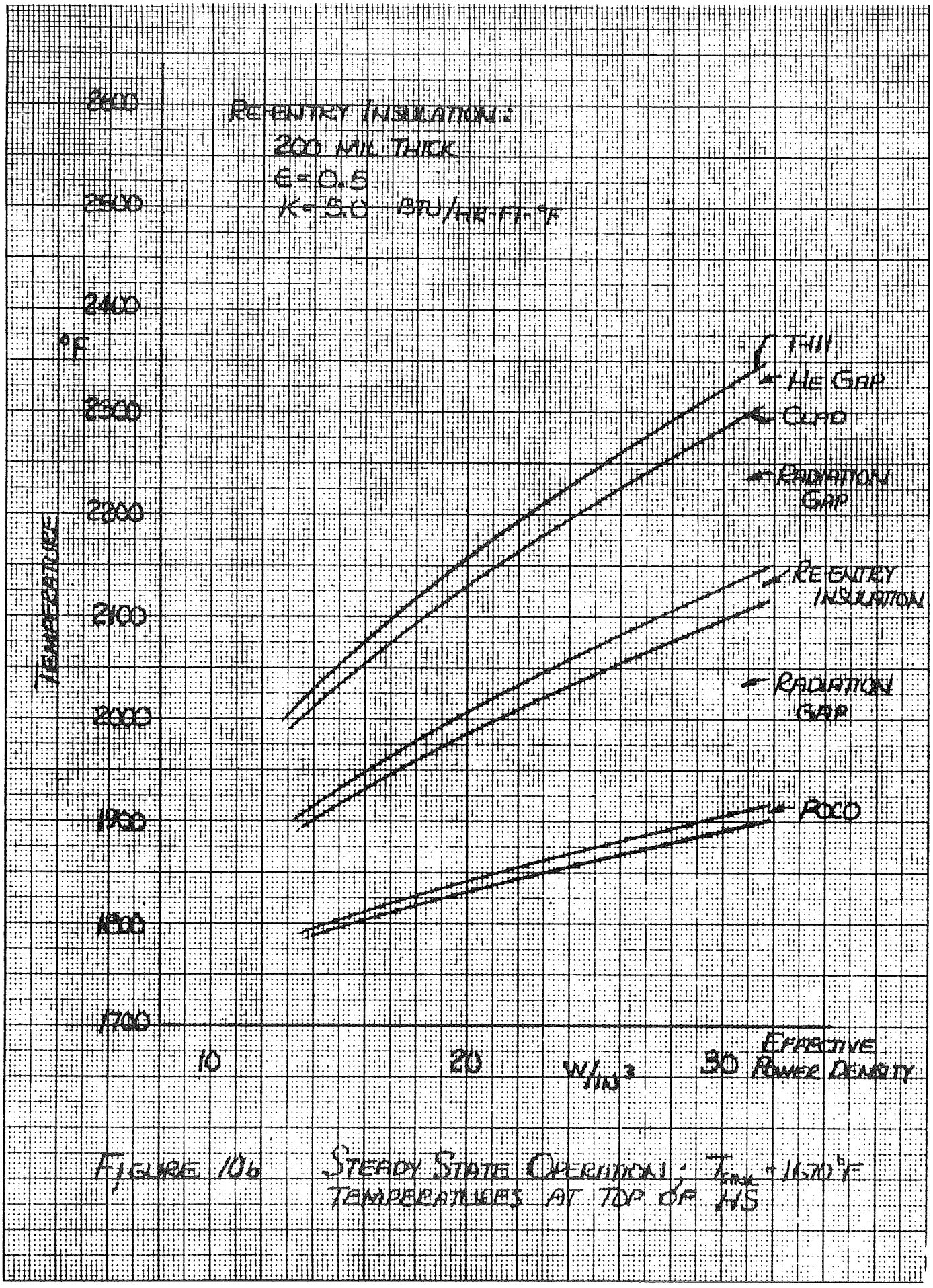

FIGURE 10b STEADY STATE OPERATION: $T_{FINE} = 1670°F$
TEMPERATURES AT TOP OF HS

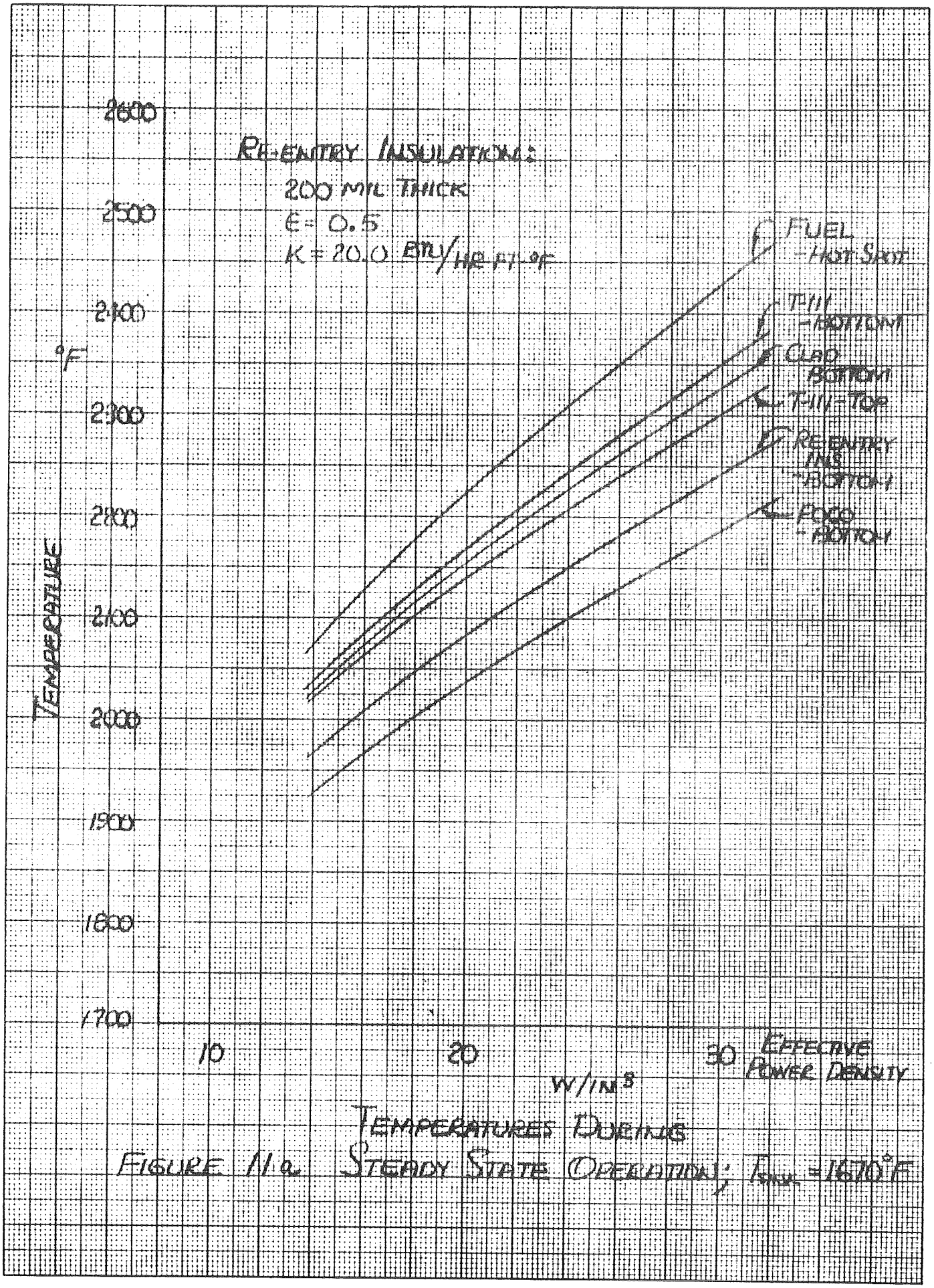

FIGURE 11a TEMPERATURES DURING STEADY STATE OPERATION; T_{MAX} = 1670°F

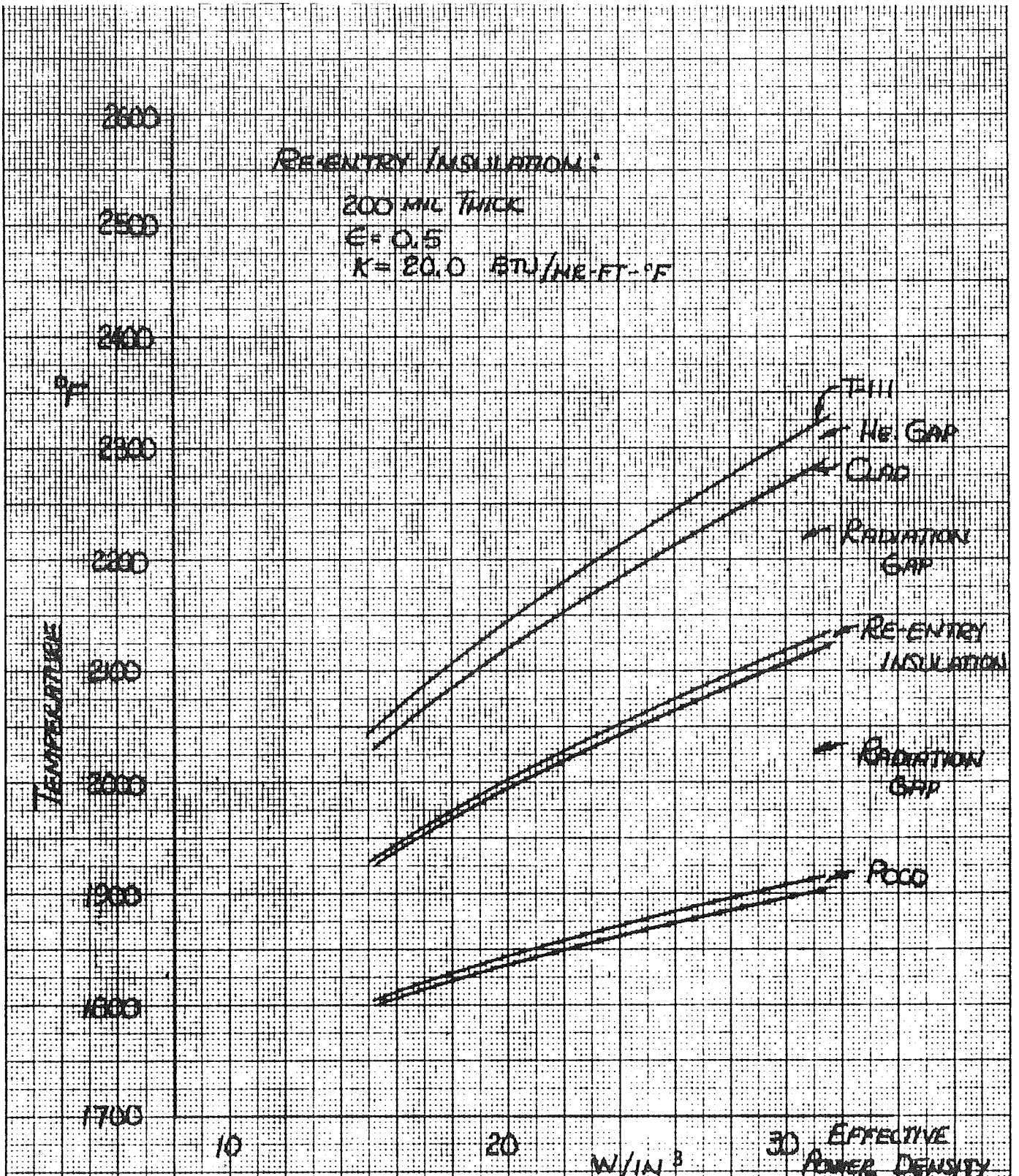

FIGURE 11 b STEADY STATE OPERATION; $T_{SAT} = 1610°F$
TEMPERATURES AT TOP OF HS

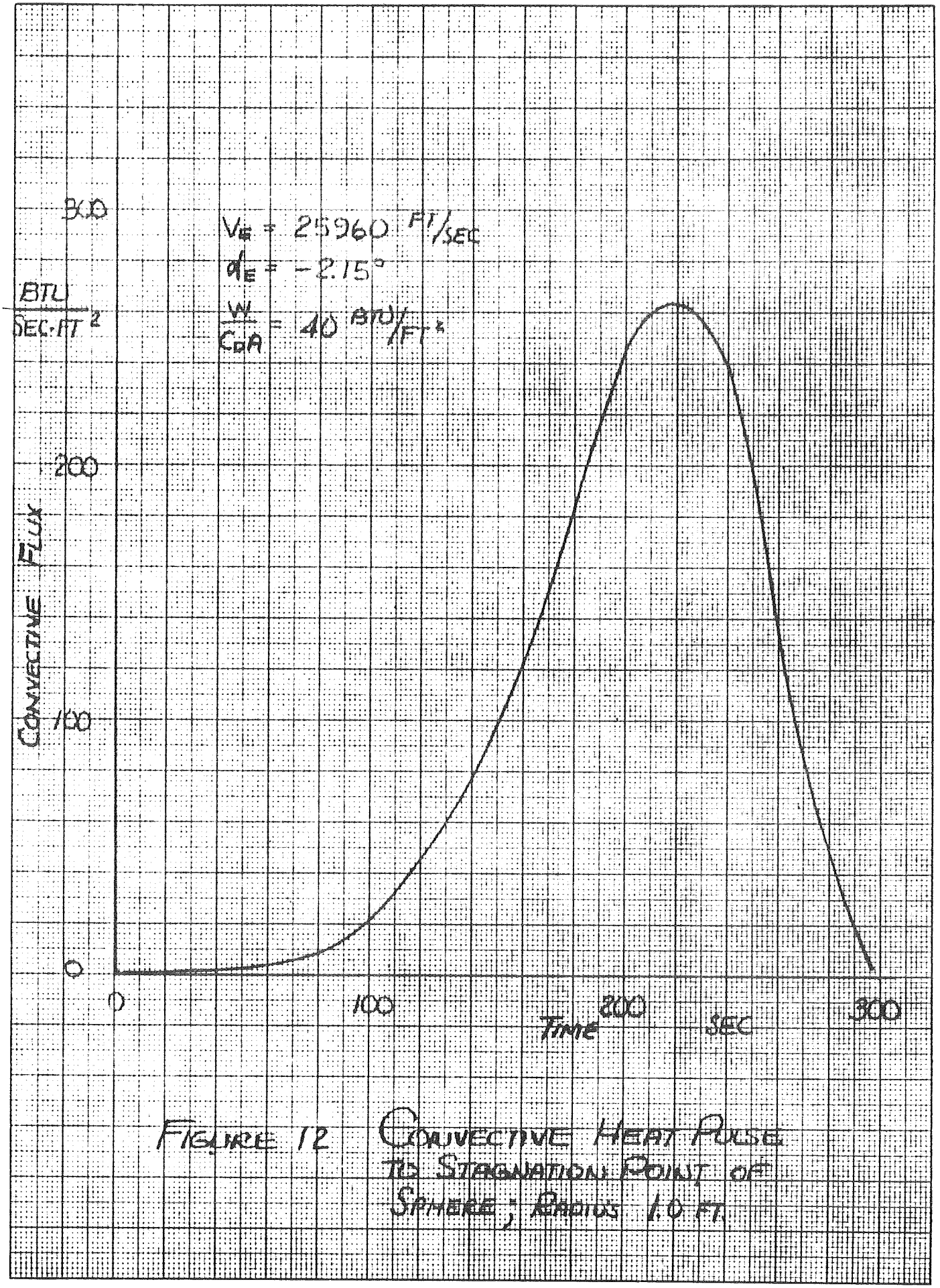

FIGURE 12 CONVECTIVE HEAT PULSE TO STAGNATION POINT OF SPHERE; RADIUS 1.0 FT.

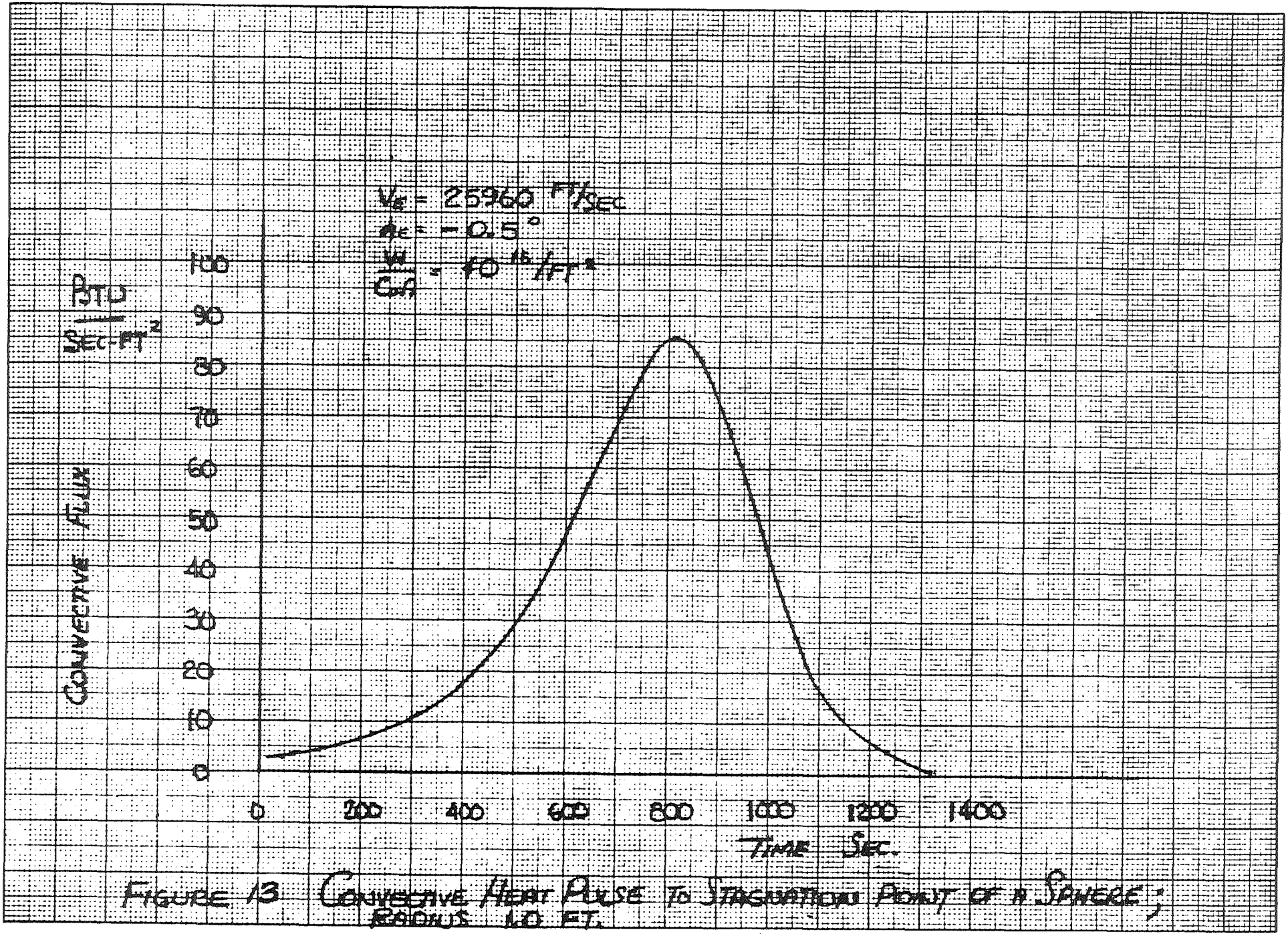

FIGURE 13 CONVECTIVE HEAT PULSE TO STAGNATION POINT OF A SPHERE; RADIUS 1.0 FT.

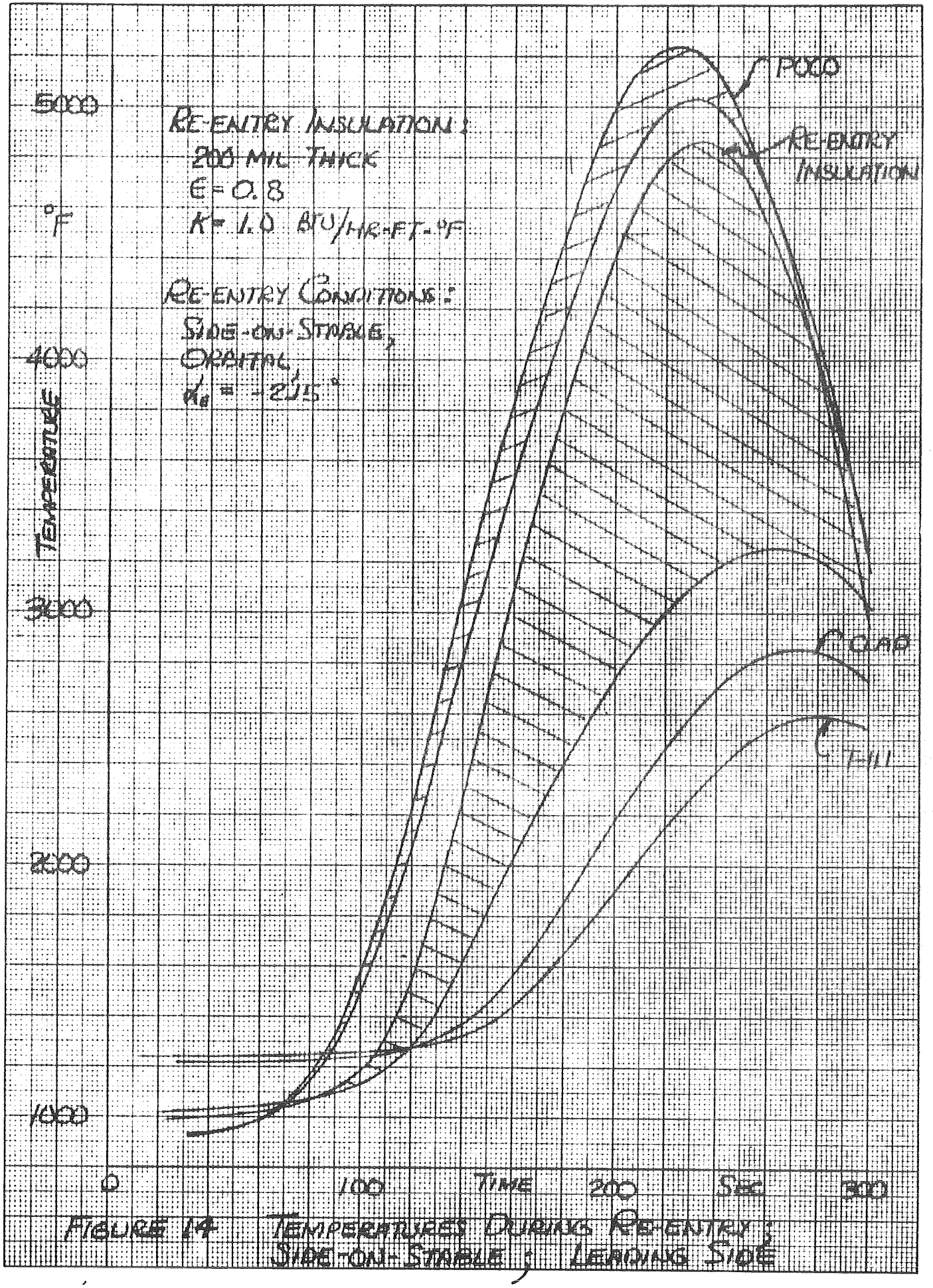

FIGURE 14 TEMPERATURES DURING RE-ENTRY; SIDE-ON-STABLE; LEEWARD SIDE

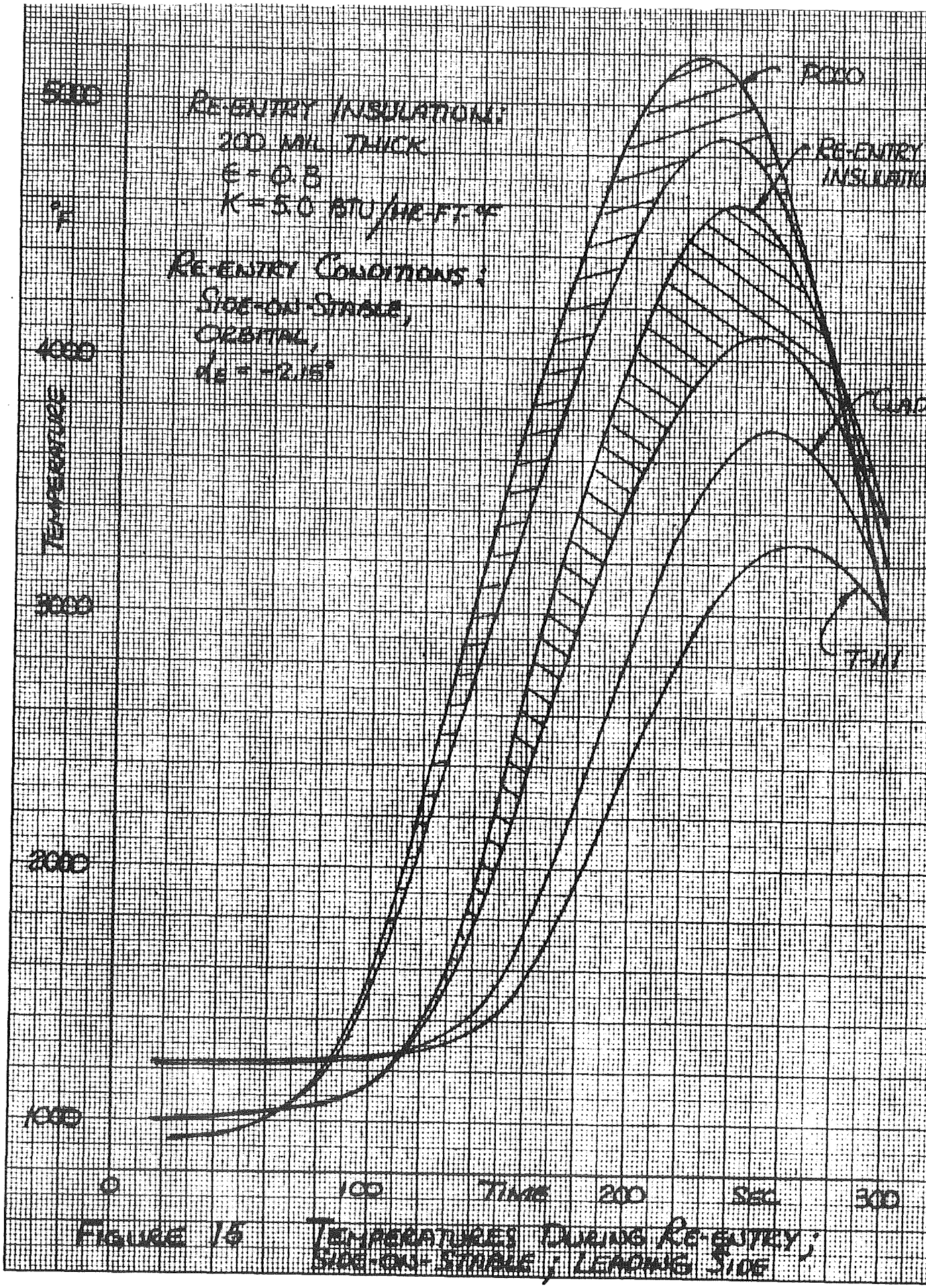

FIGURE 15 TEMPERATURES DURING RE-ENTRY; SPACE-SHUTTLE, LEADING SIDE

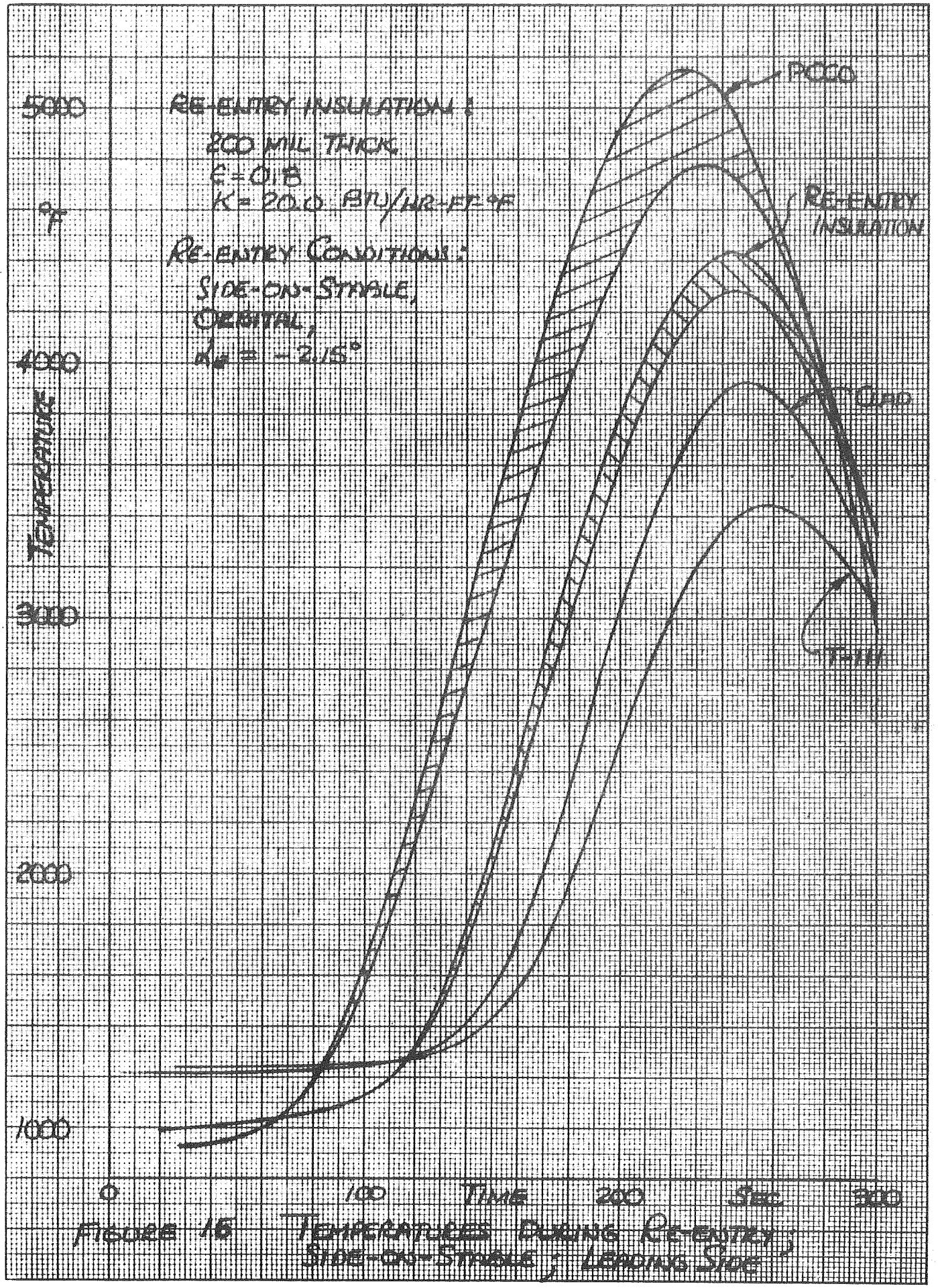

FIGURE 16 TEMPERATURES DURING RE-ENTRY ; SIDE-ON-STABLE ; LEEWARD SIDE

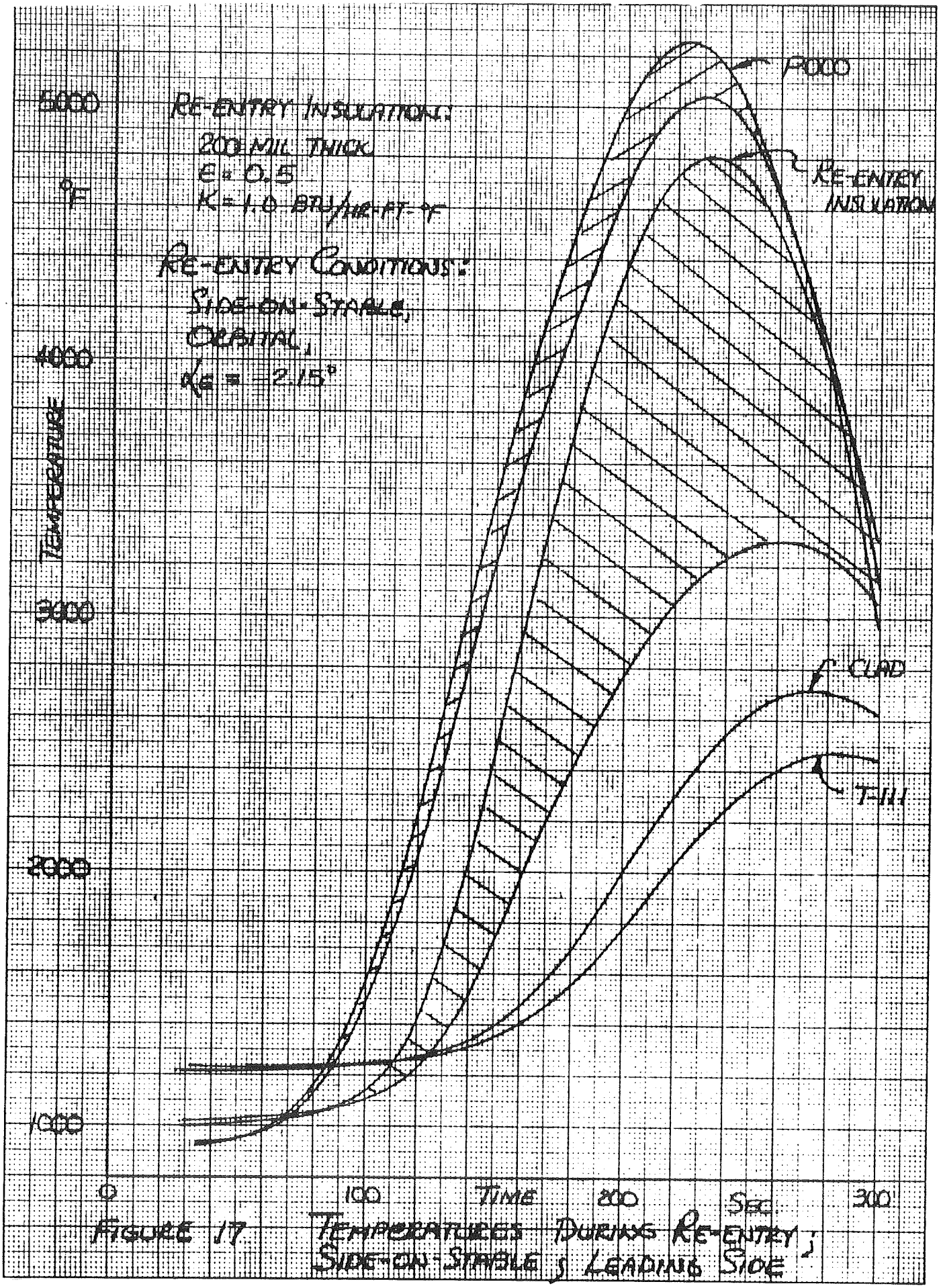

FIGURE 17 TEMPERATURES DURING RE-ENTRY; SIDE-ON-STABLE, LEADING SIDE

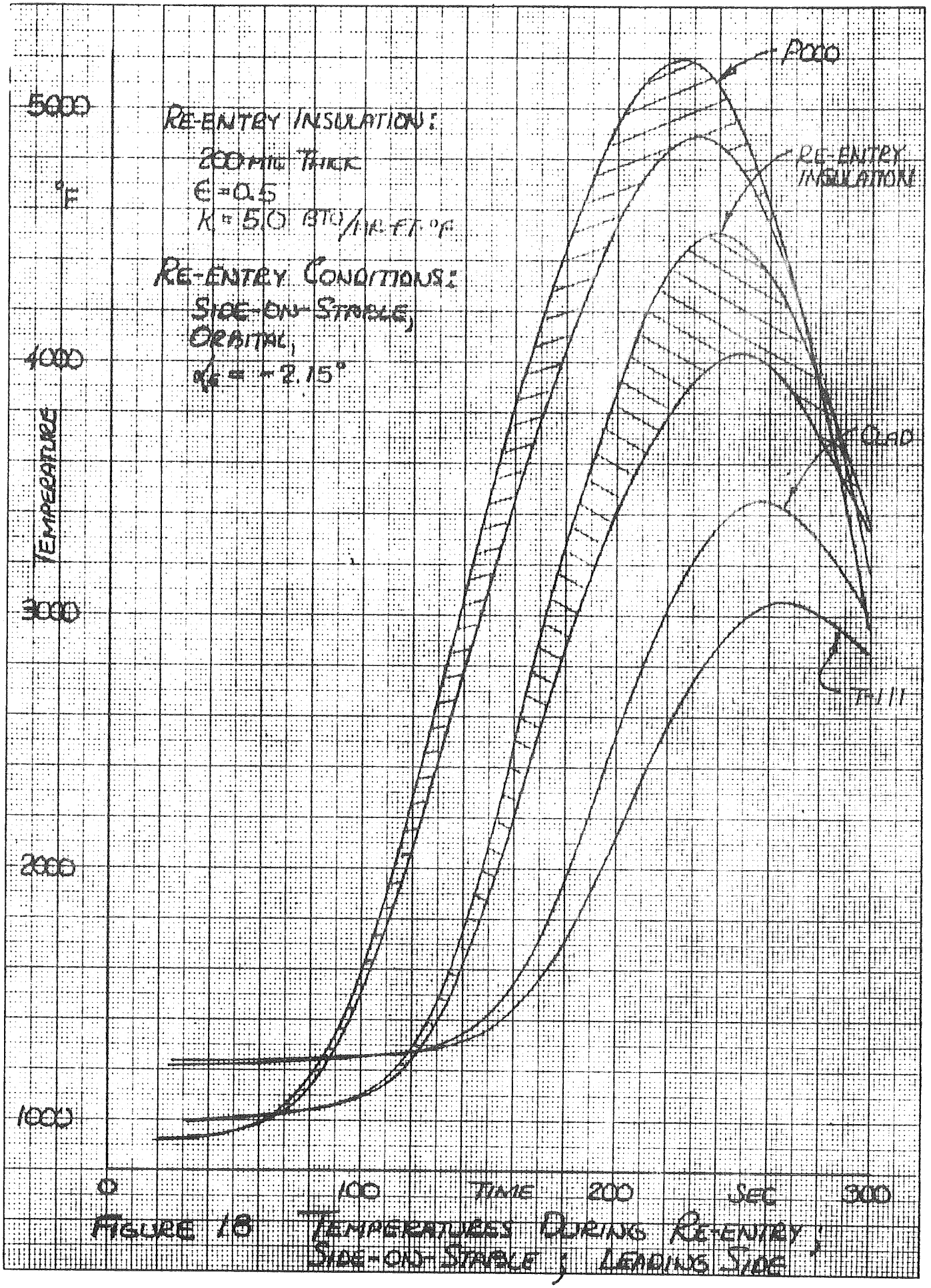

FIGURE 18 TEMPERATURES DURING RE-ENTRY, SIDE-ON-STABLE, LEADING SIDE

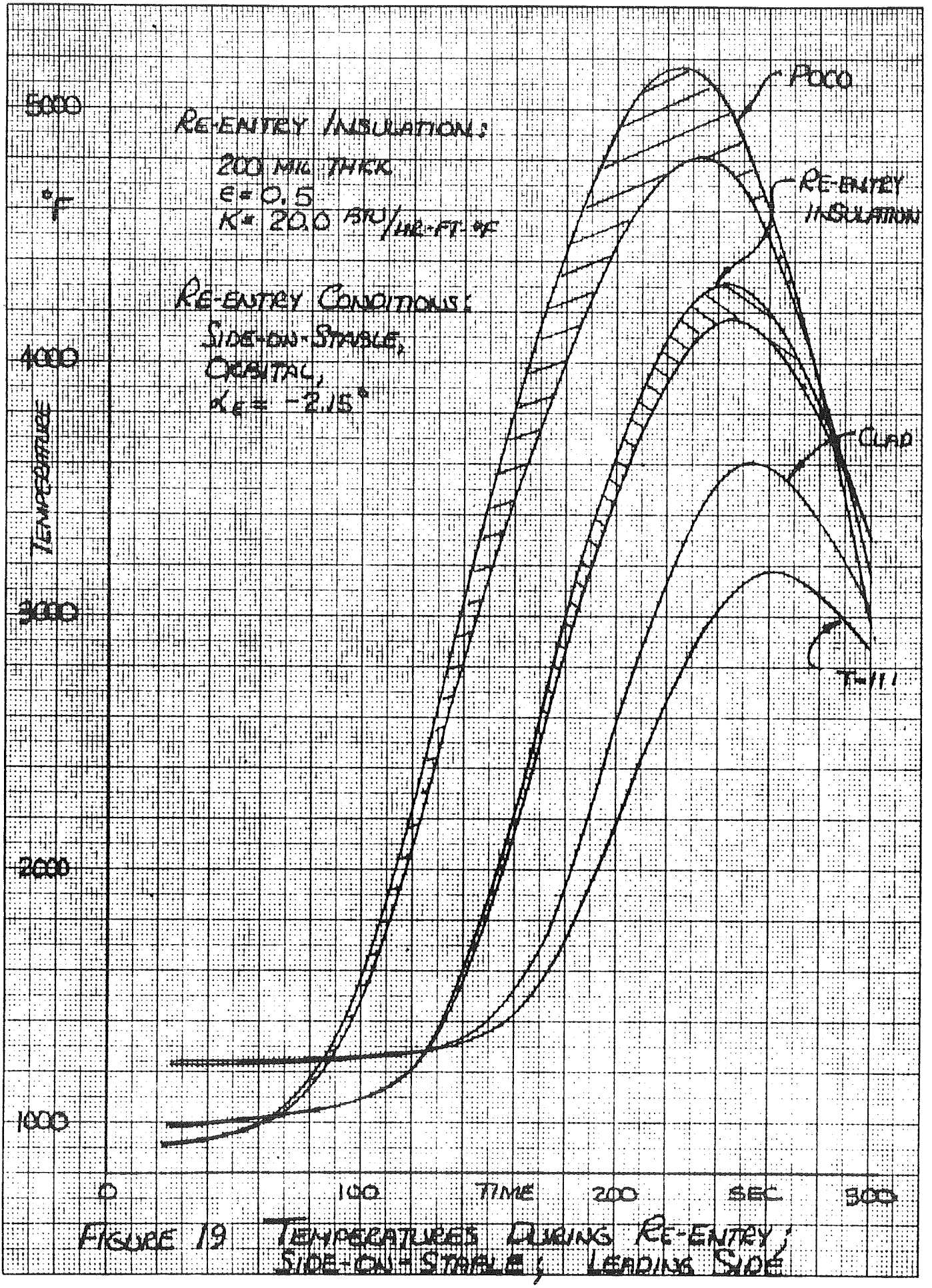

FIGURE 19 TEMPERATURES DURING RE-ENTRY, SIDE-ON-STABLE, LEADING SIDE

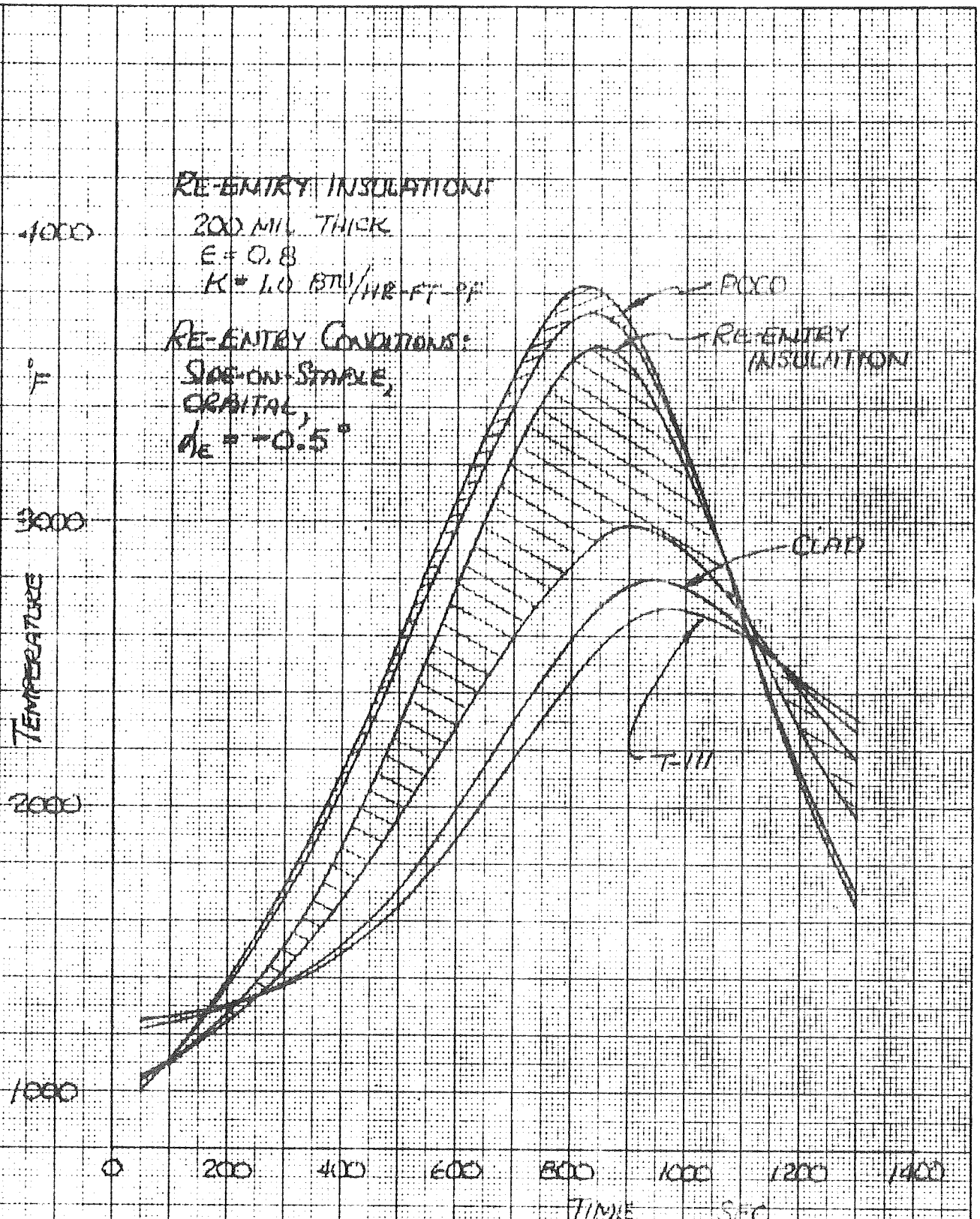

FIGURE 20 TEMPERATURES DURING RE-ENTRY; SIDE-ON-STABLE; LEADING SIDE

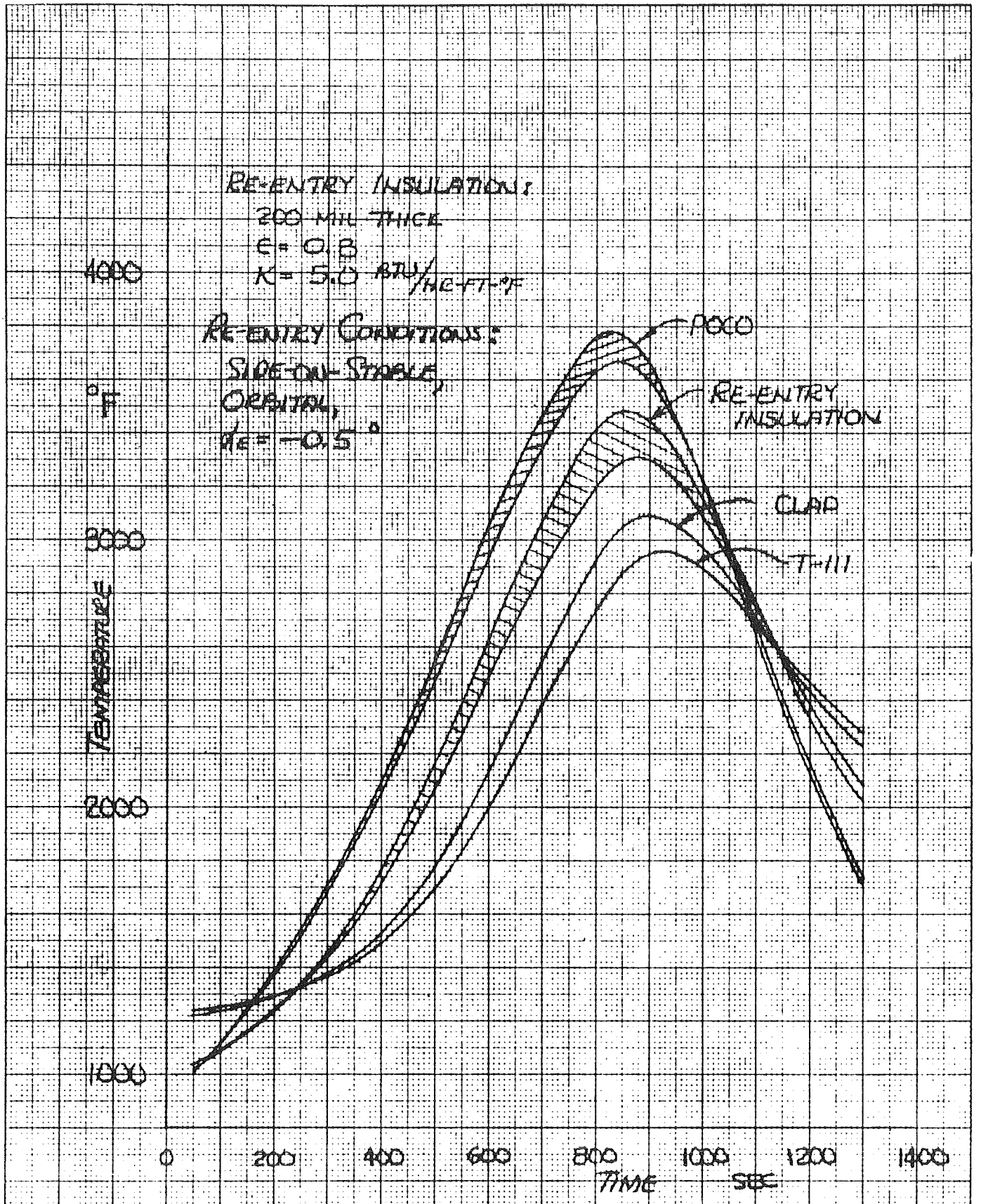

FIGURE 21 TEMPERATURES DURING RE-ENTRY; SIDE-ON-STABLE; LEADING SIDE

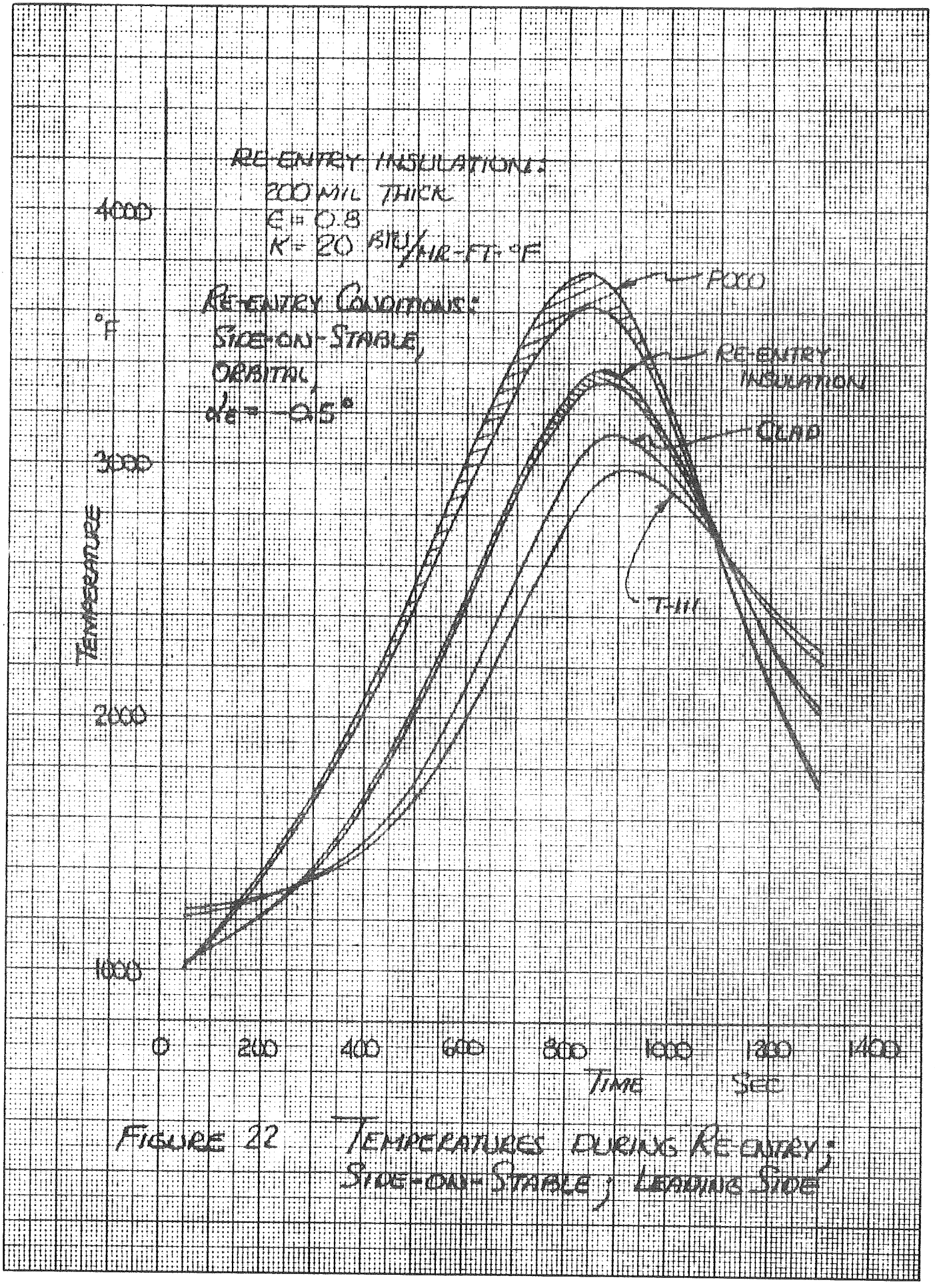

FIGURE 22 TEMPERATURES DURING RE-ENTRY; SIDE-ON-STABLE; LEADING SIDE

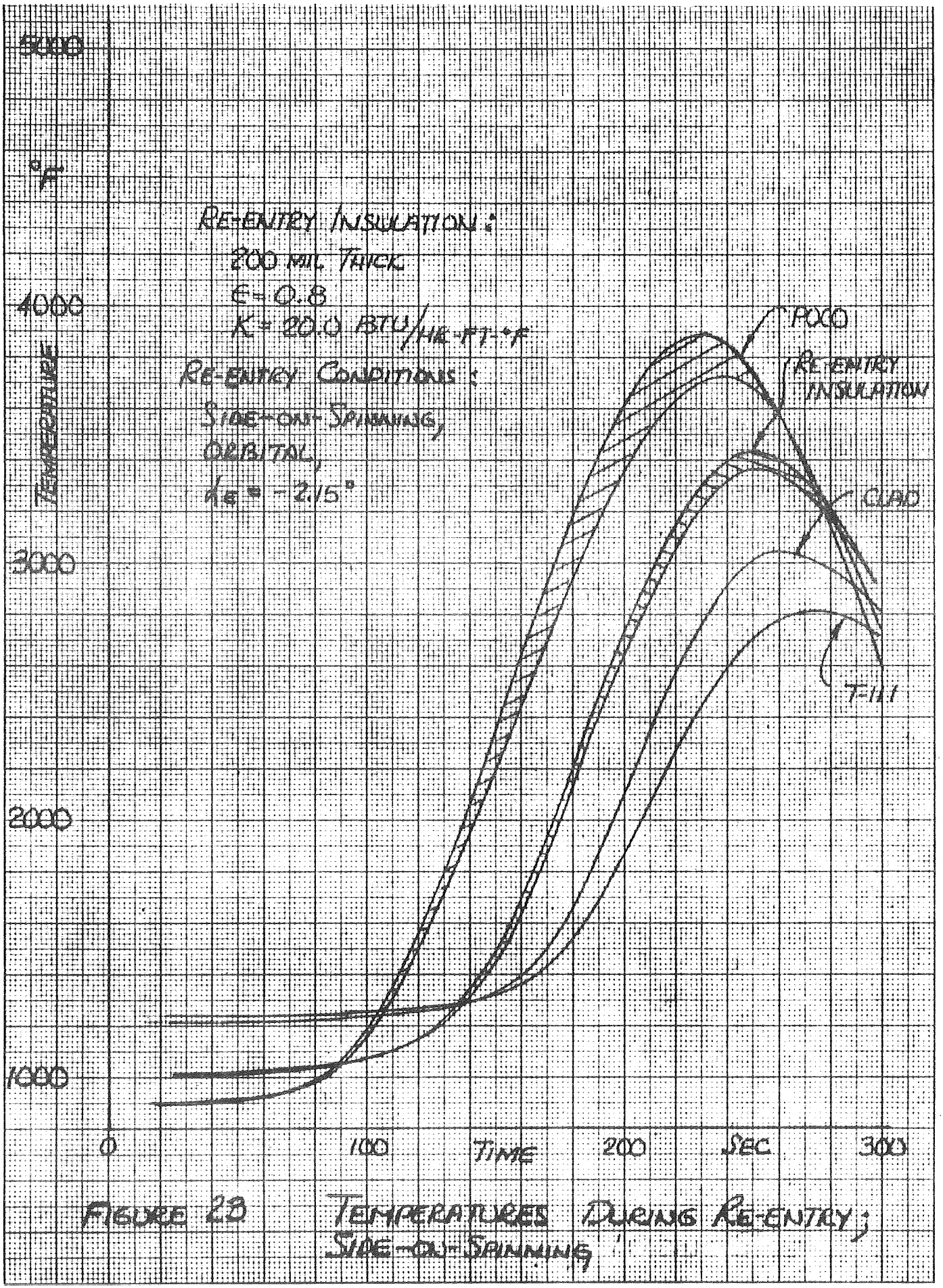

FIGURE 23 TEMPERATURES DURING RE-ENTRY; SIDE-ON-SPINNING

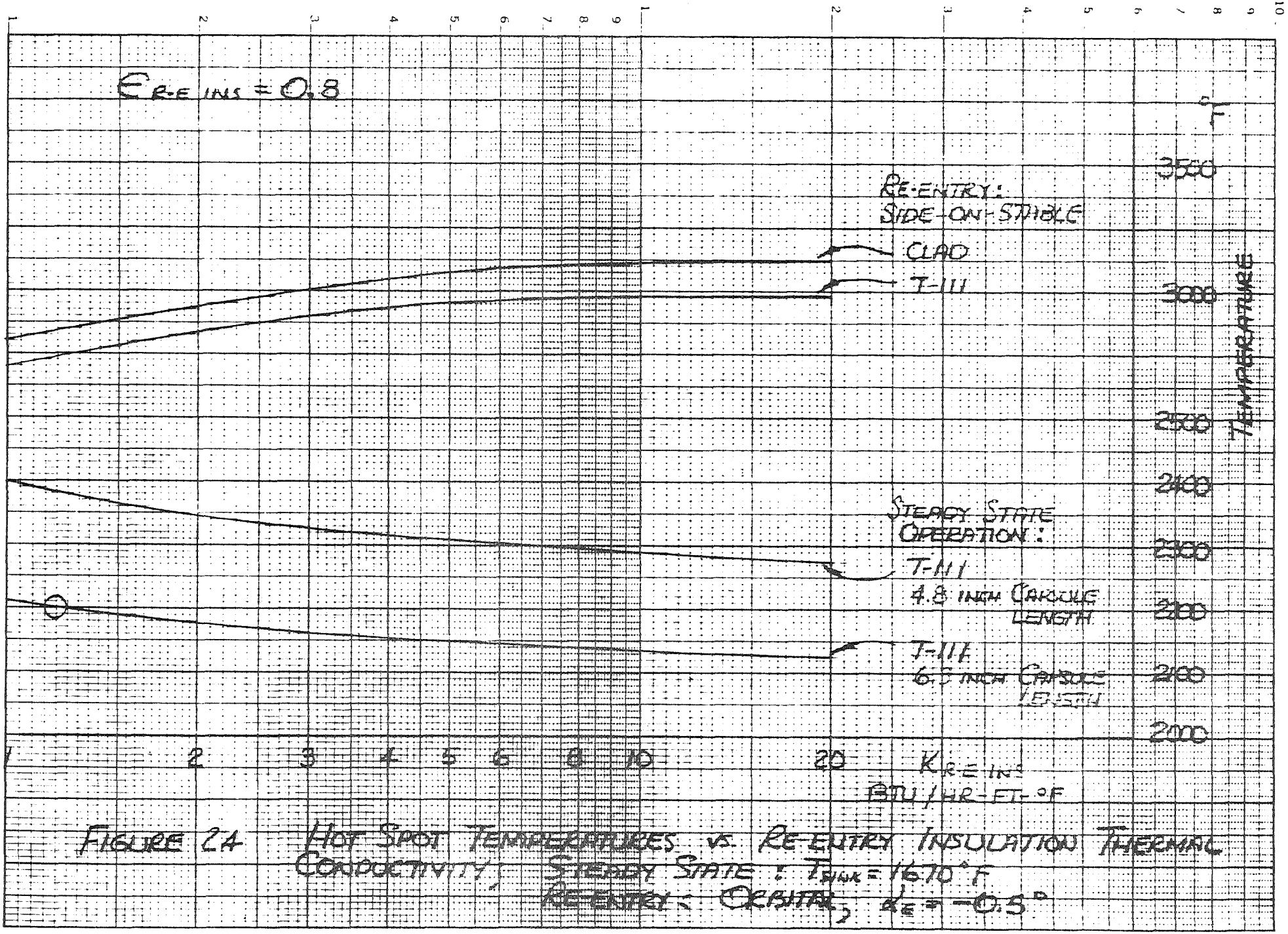

FIGURE 24 HOT SPOT TEMPERATURES VS. RE-ENTRY INSULATION THERMAL CONDUCTIVITY; STEADY STATE: $T_{SUN} = 1670°F$
RE-ENTRY: ORBITAL, $\alpha_E = -0.5°$

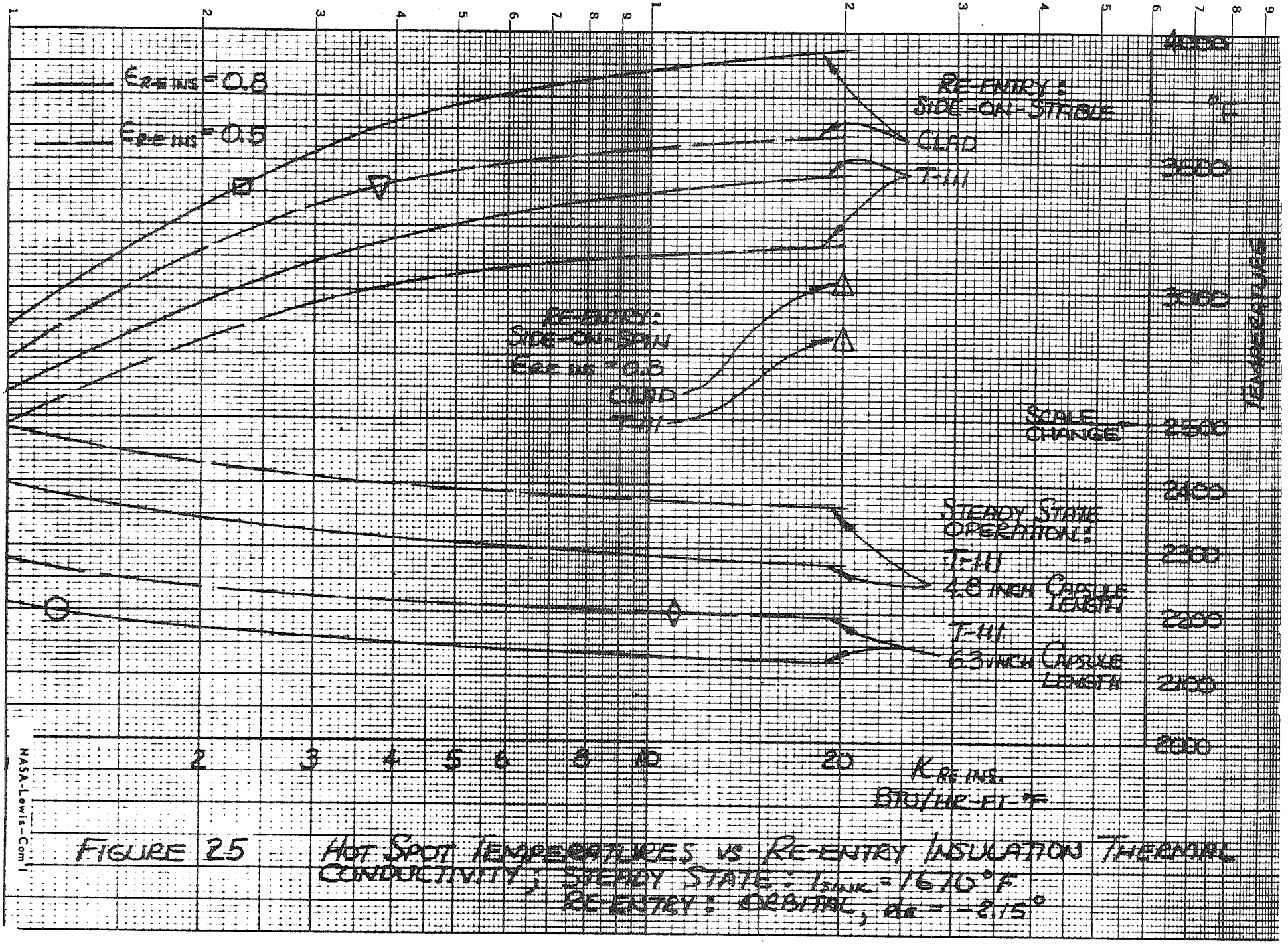

FIGURE 25 HOT SPOT TEMPERATURES VS RE-ENTRY INSULATION THERMAL CONDUCTIVITY; STEADY STATE: $T_{SINK} = 1610°F$
RE-ENTRY: ORBITAL, $\gamma_E = -2.15°$